DRA

A STUDY OF A SPACE-STATION-ASSOCIATED MULTIPLE SPACECRAFT MICHELSON SPATIAL INTERFEROMETER

NASA Contract NASW-3755

Final Report

For the Period 24 March 1983 through 30 September 1983

Principal Investigator
Robert V. Stachnik

September 1983

Prepared for
National Aeronautics and Space Administration
Washington, D.C. 20546

Smithsonian Institution
Astrophysical Observatory
Cambridge, Massachusetts 02138

(NASA-CR-175438) A STUDY OF A SPACE-STATION-ASSOCIATED MULTIPLE SPACECRAFT MICHELSON SPATIAL INTERFEROMETER Final Report, 24 Mar. - 30 Sep. 1983 (Smithsonian Astrophysical Observatory) 50 p N84-20630
G3/19 Unclas 00648

The Smithsonian Astrophysical Observatory
is a member of the
Harvard-Smithsonian Center for Astrophysics

The NASA Technical Officer for this contract is Dr. Kenneth J. Frost, NASA-Goddard Space Flight Center, Greenbelt, MD 20771.

A STUDY OF A SPACE-STATION-ASSOCIATED MULTIPLE SPACECRAFT MICHELSON SPATIAL INTERFEROMETER

NASA Contract NASW-3755

Final Report

For the Period 24 March 1983 through 30 September 1983

Principal Investigator
Robert V. Stachnik

September 1983

Prepared for
National Aeronautics and Space Administration
Washington, D.C. 20546

Smithsonian Institution
Astrophysical Observatory
Cambridge, Massachusetts 02138

The NASA Technical Officer for this contract is Dr. Kenneth J. Frost, NASA-Goddard Space Flight Center, Greenbelt, MD 20771.

TABLE OF CONTENTS

ABSTRACT

One approach to Michelson spatial interferometry at optical wavelengths involves use of an array of spacecraft in which two widely-separated telescopes collect light from a star and direct it to a third, centrally-located, device which combines the beams in order to detect and measure interference fringes. Earlier studies by us have suggested that such a system (SAMSI - Spacecraft Array for Michelson Spatial Interferometry) could be a powerful instrument for collecting extremely high resolution (10^{-5} arcsecond) spatial structure information, in the form of power spectra, for astronomical sources. High fuel consumption, however, appeared to restrict the observations to measurements along one-dimensional cuts through the source. Furthermore, recovery of information required for the reconstruction of actual images at this extraordinary resolution appeared impossible.

This report describes a modified version of SAMSI which makes use of the fuel resupply capability of a Space Station. The combination of this fuel resupply capability with our recent discovery of a method of obtaining image Fourier transform phase information, necessary for full image reconstruction, permits SAMSI to be used to synthesize images equivalent to those produced by huge apertures in space. We here discuss synthesis of apertures in the 100 to 500 meter range. Reconstruction can be performed to a visual magnitude of at least 8 for a 100Å passband in 9 hours. Data are simultaneously collected for image generation from 0.1 micron to 18 microns. In the one-dimensional mode, measurements can be made every 90 minutes (including acquisition and repointing time) for objects as faint as 19th magnitude in the visible.

I. INTRODUCTION

High optical resolution for astrophysical sources can be achieved through the use of either extremely large aperture telescopes or long baseline spatial interferometers.

In Michelson interferometry, light from a star, or other source, is collected by two widely-spaced telescopes and reflected to an interferometer located at an equi-optical-pathlength position. Contrast of the interference fringes as a function of separation of the light collectors is related in a simple way to the angular size and light distribution of the source. Figure 1 is a schematic diagram of a Michelson interferometer which includes a dispersive element allowing simultaneous multicolor observations. One possible approach to interferometry in space requires very large structures whose purpose is to establish the basic optical geometry and provide a platform for the principal optical components.

An alternative to a monolithic space interferometer is a device consisting of separate spacecraft. In such a system, two or more telescopes, aboard independent spacecraft, would simultaneously observe the same source and transmit the light they collect to a third spacecraft housing an on-board interferometer. Measurement of fringe contrast as a function of separation of the light-collecting spacecraft gives the angular size of the source. Placing the principal optical components aboard separate spacecraft, rather than connecting them by means of a very large structure, permits flexibility in selecting extremely long baselines, in this case, as much as 10 kilometers. It also implies a lower mass for the entire system and guarantees the complete vibrational isolation crucial to a large-scale interferometry experiment.

The key technical problems are associated with precision ranging, pointing, and positioning of the spacecraft, since it is necessary to equalize the optical paths through the two light collecting telescopes to within microns. Many of the required

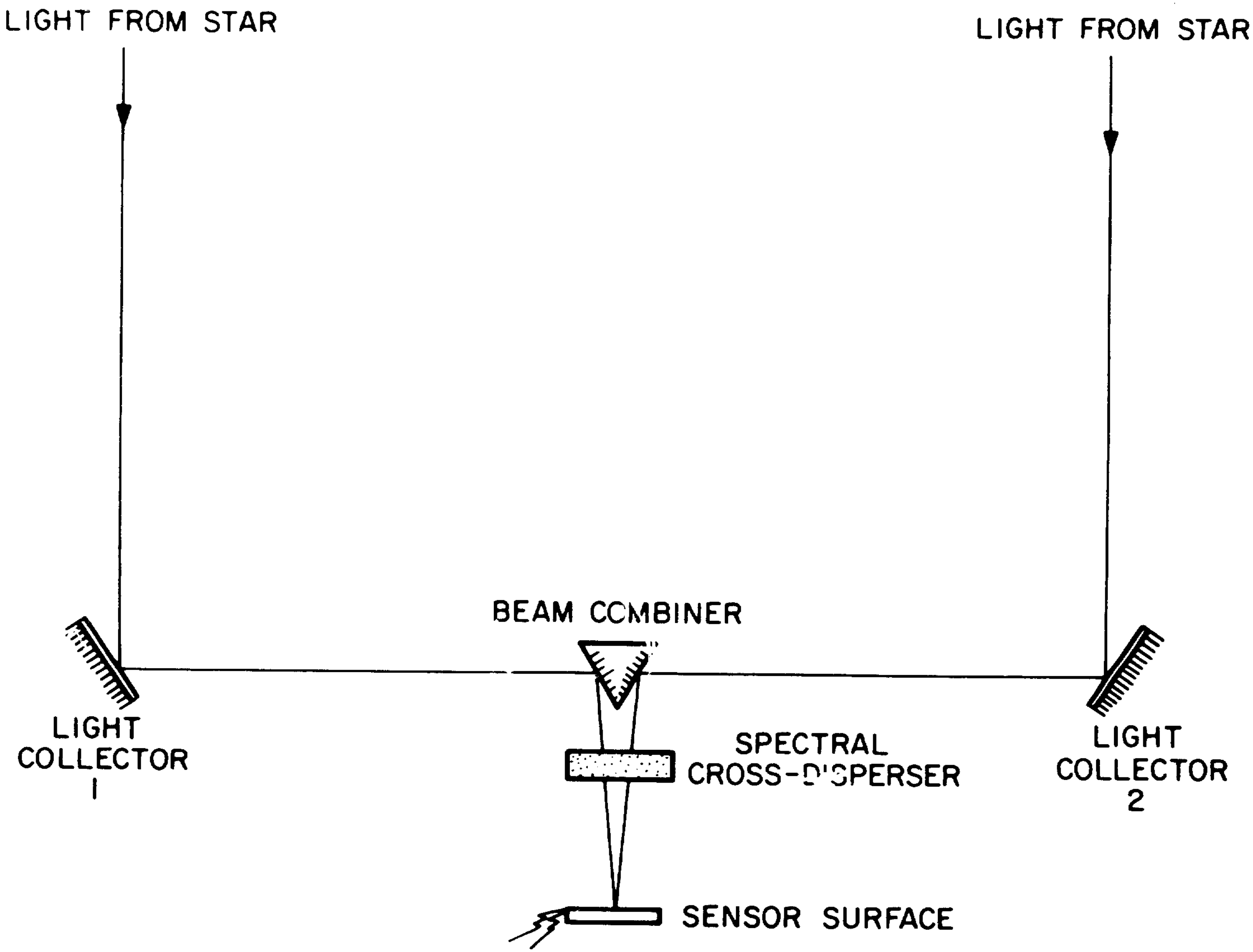
LIGHT FROM STAR
LIGHT FROM STAR
BEAM COMBINER
LIGHT COLLECTOR 1
SPECTRAL CROSS-DISPERSER
LIGHT COLLECTOR 2
SENSOR SURFACE

Fig. 1

sensing capabilities are already highly developed (Stachnik *et al.* 1983). Fine spacecraft angular position determination would be performed using an existing innovative photon-counting, star/spacecraft tracker (Papaliolios and Mertz 1982). Ranging would be done using either laser interferometry or lidar. Pathlength equalization would be done with a combination of "layered" thrusters capable of precision force application over a wide force range and a moving-mirror optical delay line in one of the two interferometer arms. Piezo-microstrain sensor/actuator pairs would provide active vibration sensing and control, and a very effective method of post-photon-detection range drift compensation exists for correction of residual errors.

In operation, the three spacecraft would deploy from the space station then move, under their own power, a suitable distance from the immediate vicinity of other space station-associated experiments. The two light collectors, each having an aperture of perhaps a meter, would point to the source to be studied and the interferometer-bearing central station would translate to the computed equi-optical-pathlength position. Small active mirrors in each light-collecting satellite would then direct narrow pencils of starlight to the central station. Aboard the central station, back-to-back telescopes would relay the beams to an on-board interferometer. Existing sensing technology allows positioning of the central station to within hundreds of microns of the true equi-path-position. At this point, the moving-mirror delay line in one optical path steps through the range of possible correct positions until fringes are sensed. Once fringes are detected, the optical delay line continues to track them as the separation between light collectors is changed. The variation of fringe contrast with separation (the visibility curve) is the basic information we require to obtain one-dimensional information in the form of a spatial power spectrum, information on the light distribution of the source. The angular resolution is set by the maximum separation of the light collectors. If this distance is 10 km, the resolution is 10^{-5} arcsecond.

Full image reconstruction also appears possible. In this mode, the spacecraft would be moved in a spiral pattern, as depicted in Figure 2, to permit sampling the entire range of spatial frequencies which would otherwise be accessible only to a single monolithic light collecting device of extraordinary size. We have, under this contract, found a way of using simultaneous observations over a very wide wavelength range, to estimate the image Fourier transform phase as well as amplitude (the latter being determined from the fringe contrast). These data are all that are required for image reconstruction. Available array sensors used in detecting the fringe patterns would allow recovery of high-resolution images over a wavelength interval extending from 0.1 to 18 microns, in narrow spectral passbands. Because full image reconstruction is time-consuming (9 hours, for complete sampling over a 100-meter spiral) and most appropriate to brighter objects (8th magnitude), fainter sources (19th magnitude) would be observed by making one dimensional fringe contrast measurements, to obtain angular diameters. This dual mode of operation is an important characteristic of the system.

The spacecraft would be under continuous active position control and the overall observing efficiency of the interferometer would depend on positioning the spacecraft as rapidly as is consistent with the limitations of the thrusters and sensing systems. At present, it appears that the combination of thrust and efficiency requirements in the propulsion system mandate principal reliance on liquid hydrogen/liquid oxygen thursters, for which fuel use, because of the 100% duty cycles, would be comparatively high despite their high specific impulse. It is in this connection that the association with the space station becomes vital. The space station would serve as a refueling facility for the otherwise autonomous system of spacecraft. At present, a European group (Laboyrie *et al*. 1982; Stachnik and Labeyrie 1984) is exploring a very similar system. Wtihout the availability of a refueling facility, however, they are forced to rely on a solar sail design for which the forces and, consequently, observing efficiency, may be nearly four orders of magni-

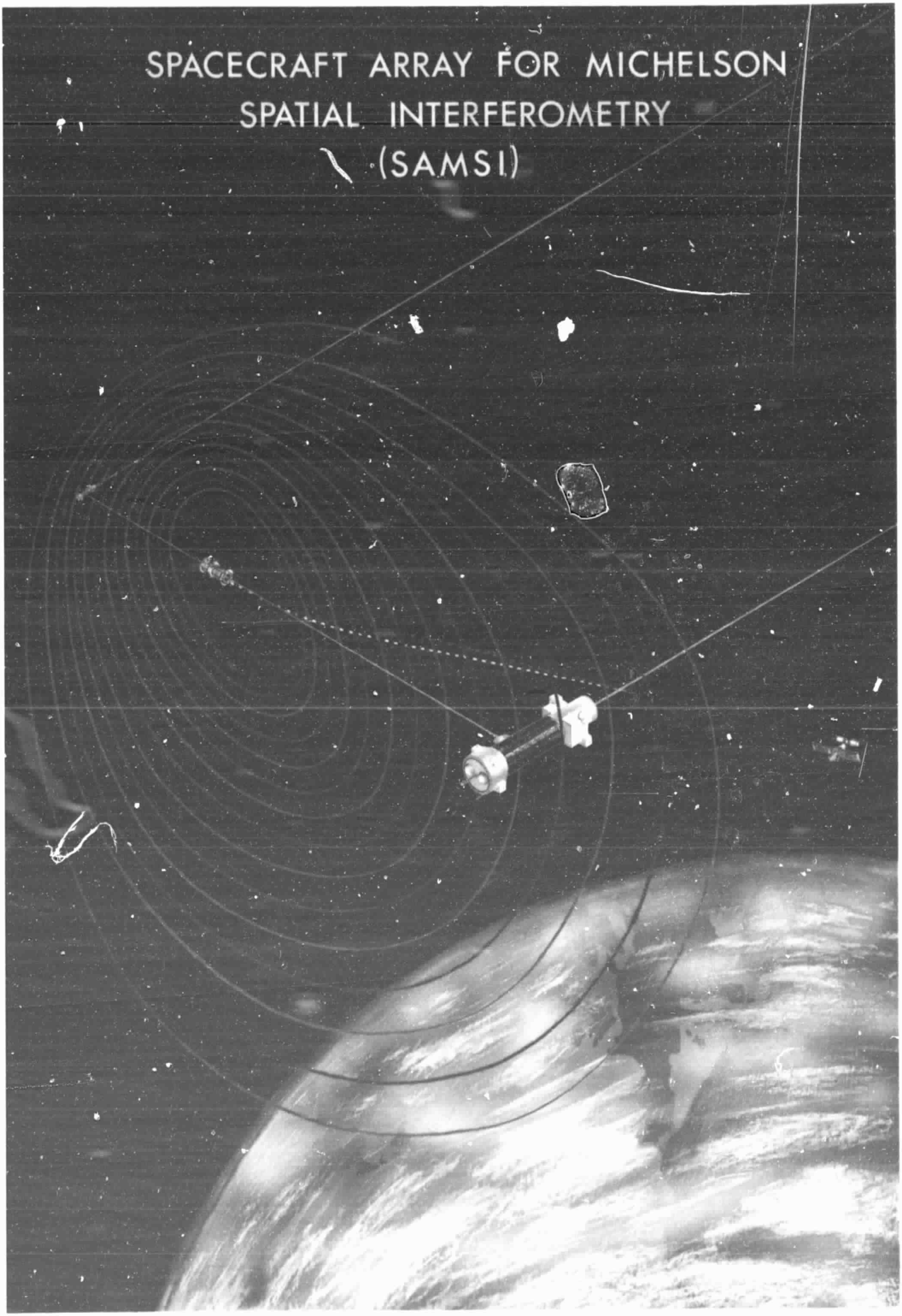
SPACECRAFT ARRAY FOR MICHELSON
SPATIAL INTERFEROMETRY
(SAMSI)

tude smaller.

Continuous, rapid motion of the spacecraft, made possible by periodic refueling, would render a multiple spacecraft interferometer an extremely powerful and versatile scientific instrument. It would be capable of obtaining either large numbers of one-dimensional measurements or a lesser number of two-dimensional images. The resolution would be a function of observing requirements since imaging baselines of hundreds of meters or one-dimensional baselines of tens of kilometers will not always be needed. For special objects, unusually large or small baselines may be employed.

The resolution achievable with the 100 m imaging baseline we emphasize here is at least 10^{-3} arcsecond in the visible. This is three orders of magnitude greater than is typical of routine earth-based measurements and a factor of 40 greater than is expected from Space Telescope. In the alternate, one-dimensional mode, 10-km baselines are possible and, due to the existance of advantageous orbital configurations, the corresponding 10^{-5} arcsecond resolution observations can be made at a rate of 16 sources per day.

In what follows, we describe a design based on an earlier low-thrust, nonrefuelable system for which actual imaging did not appear possible. This earlier device is described in Stachnik *et al.* (1983). Parts of Sections II and VII of this report are largely taken from that source.

II. OPTICAL DESIGN

In order for the interferometer in the central station to detect and measure fringes, the central station must be near enough to an equi-optical-path position that a delay line in one of the optical paths can make both paths equal to within a few wavelengths. An optical delay line is a device which (in the simplest case) uses a moving mirror to adjust optical path length. In general, the focus of equi-optical-path positions is a surface defined by the condition that the difference between the distance to light collector number 1 and the distance to light collector number 2 is equal at every point. This surface is a hyperbola of revolution about the axis joining the two light collectors.

Figure 3 is a schematic diagram of the central station. It consists of two back-to-back telescopes acting as receivers for starlight redirected by the collecting telescopes. The back-to-back central station telescopes are also used to transmit and receive laser light, which bounces off retroreflectors on the light collecting telescopes, for use in position sensing. The data and position sensing beams pass through the same optical systems and may be separated either spectrally or temporally.

Initial acquisition of the fringes involves coarse positioning of the central station with a subsequent fringe search over the region of uncertainty. A combination of distance measurement between spacecraft and angle measurement would allow positioning of the central station to within much less than ± 0.5 mm. In the following paragraphs, we discuss factors bearing primarily on initial fringe acquisition.

In order to achieve ± 0.5mm pathlength equality, for instance, over a kilometer 0.1 arcsecond tracking accuracy is required, as is the ability to measure distances to within fractions of a millimeter. Lidar distance measurement to better than ± 0.5mm has been demonstrated (Querzola 1979) and the existence of an integral dispersive element in the data collection system largely eliminates the data beam/locator beam cross-talk problem. Although it is angle tracking that sets the limits on determination of optical path length, far higher distance measurement accuracy could be achieved using interferometry rather than lidar. Furthermore, use of a multicolor laser interferometer permits absolute distance determination. A device claiming one part in 10^9 accuracy is described by Bien *et al.*(1981). 0.02μ accuracy for modulo one-meter absolute distance measurement has been demonstrat-

CENTRAL STATION

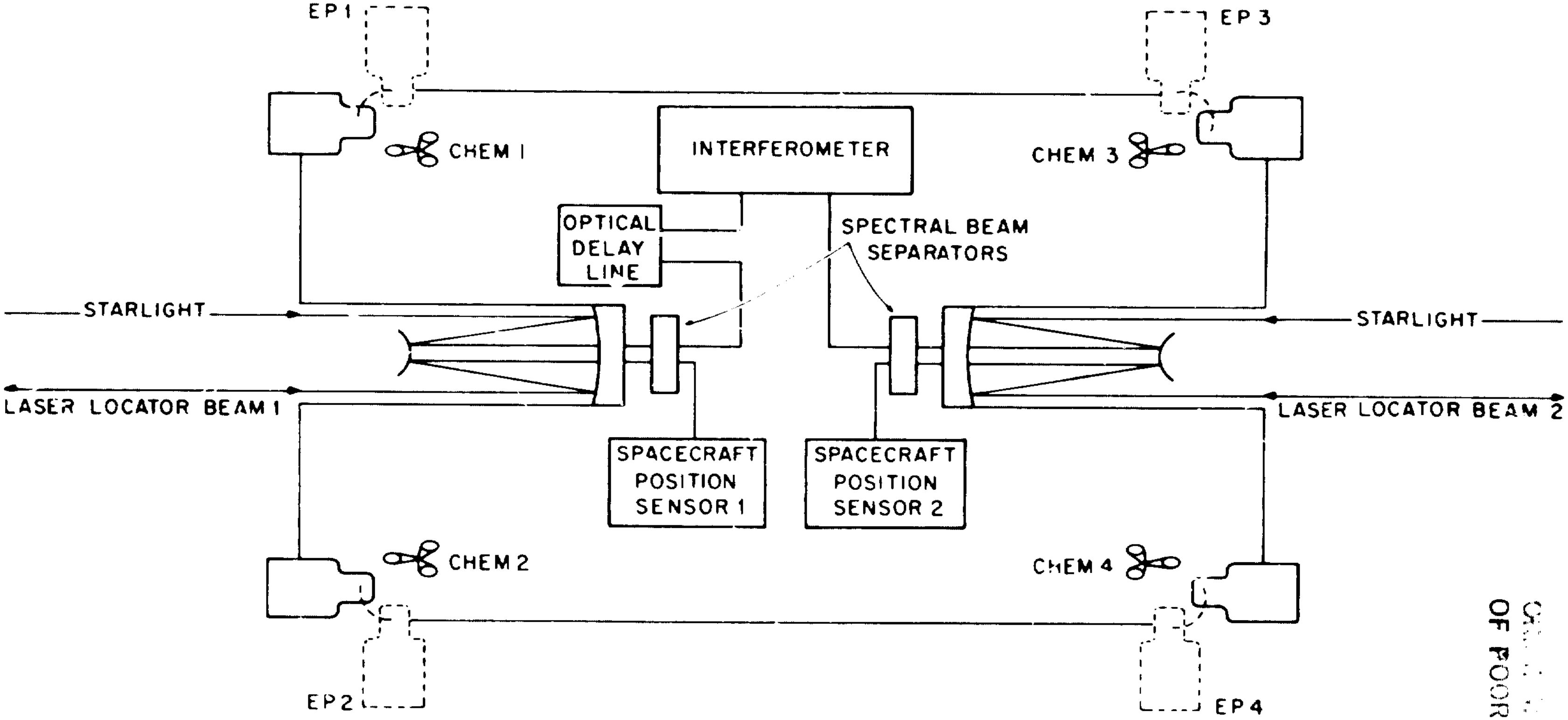

EP: GIMBALLED ELECTRIC THRUSTER (ION ENGINE)

CHEM: CHEMICAL THRUSTER (HYDRAZINE)

Fig. 3

ed using a 6-color laser interferometer (Bourdet and Orszag 1979). The modulo 1-meter ambiguity is easily resolved with either lidar or radar. Coarse and emergency location would also be done with radar.

With highly accurate distance determination possible, the principal requirements for fringe position prediction are precise spacecraft tracking and large angle measurement. 0.04 arcsecond (2mm at 10km) tracking in space applications was reported 10 years ago in Air Force Program 405B (Elson 1973). If the back-to-back central station telescopes have 20 cm diameters and operate at the diffraction limit in the visible, 0.1 arcsec tracking (5mm at 10 km) requires position sensing to one-fifth of the diffraction limit. SOT, the 1-meter Solar Orbiting Telescope, is designed for tracking to an accuracy 0.2 times its diffraction limit on a far more difficult object, the Sun (Dunn 1980). Space telescope is designed for tracking to 0.15 times its diffraction limit (Jones 1979). Spacecraft pointing would be done with the usual combination of control moment gyros and momentum dumping by means of thrusters. The attidue of the three spacecraft with respect to an external coordinate system would be obtained from measurements of light collector positions against the grid of background stars made at the central station.

Once located, the fringes must be tracked. Analyses of tracking and measurement errors arising for photon-noisy fringes are found in Kibblewhite (1979) and in more detail by Hardy and Wallner (1978). An analysis of signal-to-noise in Michelson interferometry also appears in Tango and Twiss (1980), and in Greenaway (1979).

Figure 4 shows one of the light collector satellites. This design could, in principle, be replaced by a large flat, or, for cases where the source is far off the normal to the line along which the three spacecraft are displaced, a pair of flats. Substitution of large flats, however, seems to offer no advantage of cost or simplicity of design or fabrication, and requires larger telescopes on the central station

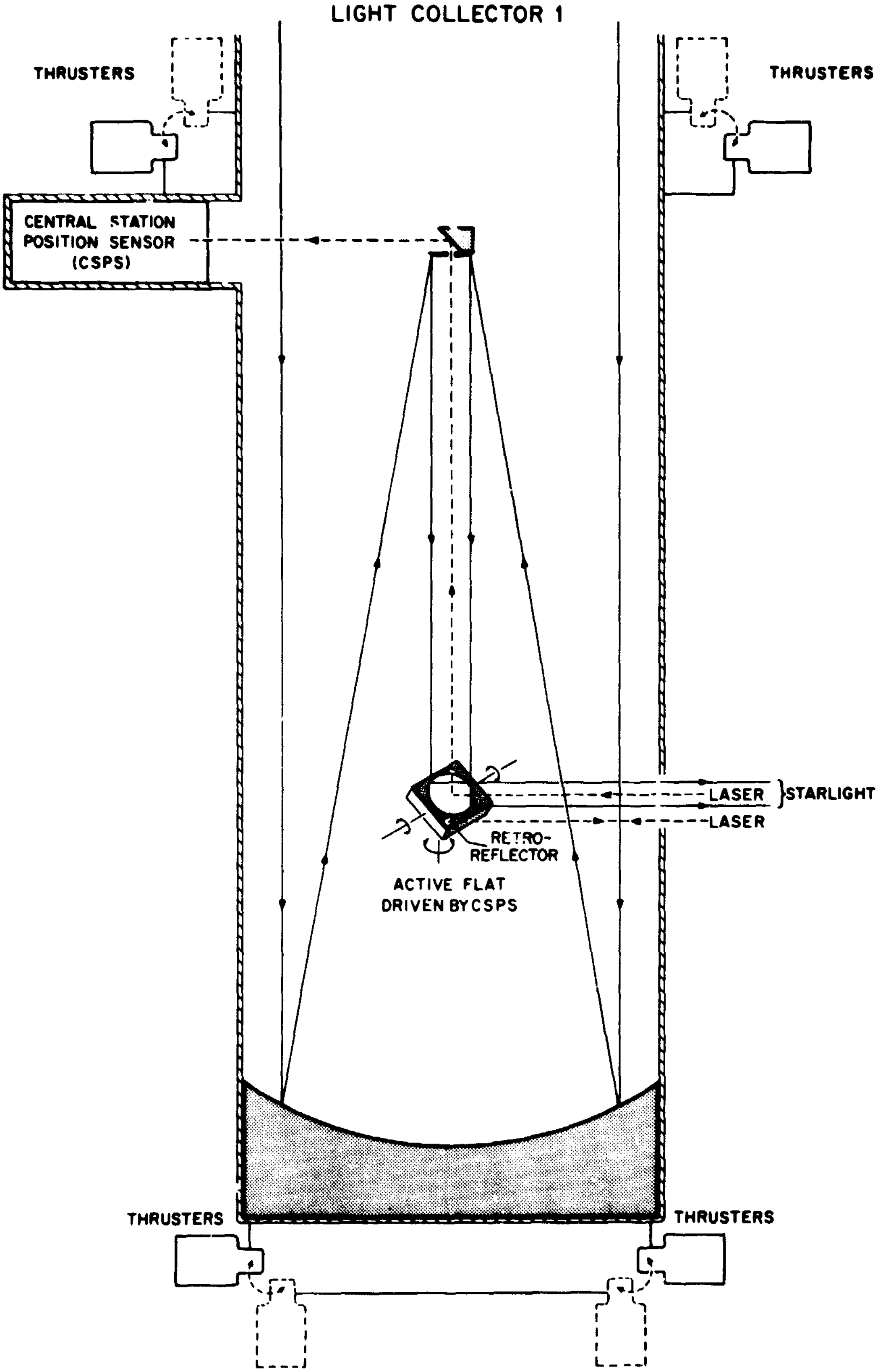
LIGHT COLLECTOR 1
THRUSTERS
THRUSTERS
CENTRAL STATION
POSITION SENSOR
(CSPS)
LASER
STARLIGHT
LASER
RETRO-
REFLECTOR
ACTIVE FLAT
DRIVEN BY CSPS
THRUSTERS
THRUSTERS

Fig. 4

to accept the unconverged beams.

The light collectors must be diffraction-limited optical systems and require full three-axes stabilization to, perhaps, a fifth of a diffraction resolution element. (The diffraction limit is 0.1 arcsec for a 1-meter aperture.) An acquisition and tracking system is required to control the small flat directing light from the collecting telescope to the central station, with fine tracking based on signals transmitted from error sensors on the central station.

A sample optical layout for the central station including a scheme for pointing and range error signal generation, appears in Figure 5. In this system, lidar, rather than interferometry is used for ranging. A legend describes the basic optical components. In the diagram, quad cells are four-element position sensing devices, which generate corrective error signals if the detected signal is not balanced among all four sensors. Nutating mirrors or other systems may prove more sensitive. Elements marked "active mirrors" are tip-tilt devices except for the delay line mirror which has linear motion only. The dichroics transmit laser light and reflect light from the source to be studied. Coarse pointing may be done with small motions of the two central station telescopes. Fine pointing is done with smaller active mirrors.

A pulsed laser in each of the two tracking and pointing systems periodically transmits pulses outward, through the active optical system, in the direction of the light collector it is to track. We shall consider the case of system number 1, tracking light collector no. 1.

Part of the outgoing pulse is picked off (here by the back surface of the dichroic) and relayed to the ranging pulse sensor, D1. The pulse is returned to the central station by a retro reflector mounted on (possibly at the center of) the active flat on light collecting satellite no. 1. The pulse returns to detector D1 after passing through the delay line, through the dichroic, and reflecting off one beam-

CENTRAL STATION—OPTICAL SCHEMATIC

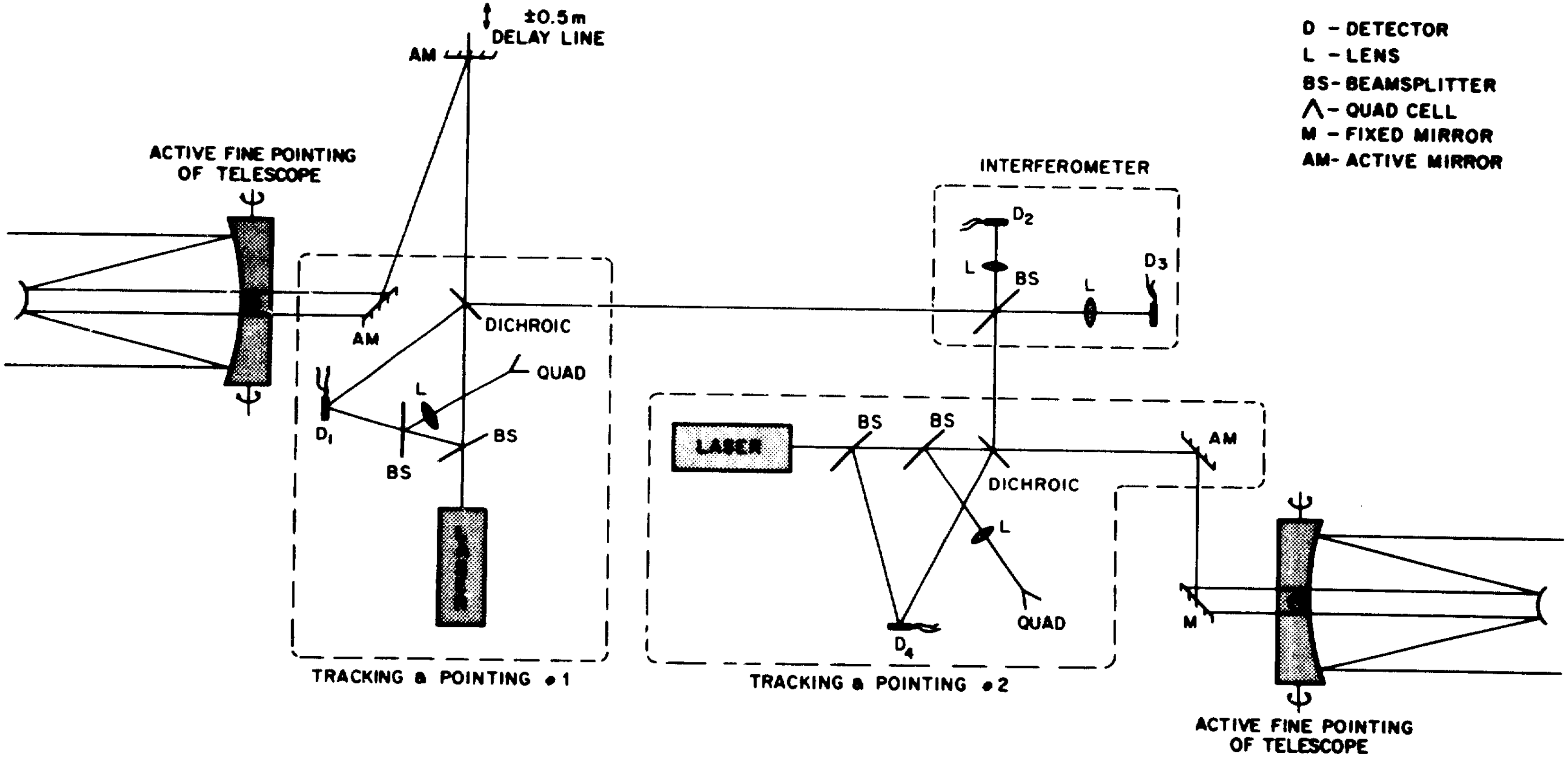

Fig. 5

splitter then passing through another. The difference between the distances obtained from systems 1 and 2 is compared with that calculated for the expected location of the fringes and the central station is moved as appropriate. Fine adjustment is made by means of the delay line. The component of the return pulse reflected off the second beamsplitter goes to a quad cell or a similar device to generate pointing error information.

The sensing beams are coincident with the data beams for which we wish to obtain interference. The data beams are reflected off the front surfaces of the dichroics and into an interferometer. The interferometer in Figure 5 is shown schematically. In fact, a modification of Michelson's original method of interfering the beams would be used. The beams would be brought together at a narrow angle after passing through a dispersive element permitting simultaneous observation of the resulting fringes over a wide range of wavelengths. Figure 6 shows the fringe patterns falling on a set of 4 array detectors covering a spectral range between 0.1 and 18.0 microns.

An extremely important sensor characteristic, now demonstrated at visible wavelengths (Papaliolios and Mertz 1982) is image detection in a photon cataloguing mode. Since certain photon-counting array sensors record detected photons as an x, y, t catalog, t being the time of detection, it is possible in the case of a regularly changing pathlength (fringe drift) error, first to detect the photons, then record them as times and addresses, perform drift compensation in software, and finally, use the new positions to generate a drift-corrected fringe pattern and measure a contrast. If the absolute drift rate is unknown, different values are tried with the goal of optimizing contrast. Furthermore, observed changes in velocity between integration intervals can be used to model accelerations affecting contrast measurements during an interval.

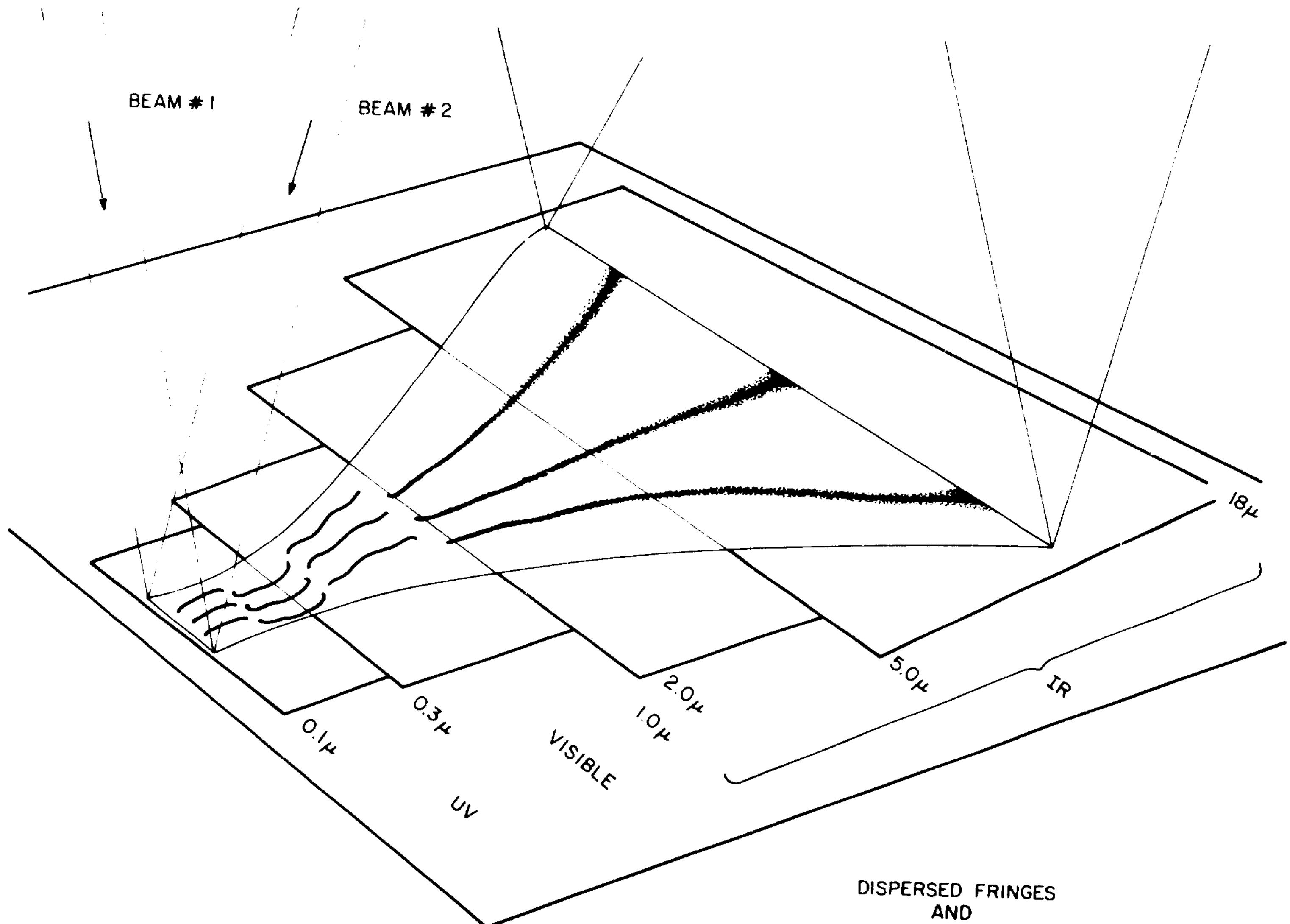

DISPERSED FRINGES
AND
SENSOR ARRAYS

Fig. 6

III. OPERATIONAL CHARACTERISTICS AND ORBITAL MOTION

In operation, the three spacecraft comprising SAMSI would deploy from Space Station powered by thrusters capable of producing a net thrust of 0.5 newton in any direction. This thruster size was chosen to guarantee station-keeping for 1000 kg. spacecraft in a low earth orbit at all orientations, and for separations of several hundred meters (after Columbo *et al.*, 1976). An estimate of 1000 kg per 1 meter telescope/spacecraft appears safe since cube-law scaling from the 10600 kg mass of the 2.4-meter Space Telescope, suggests a mass of 770 kg. The mass of IRAS, with a 60 cm aperture, is 812 kg. Of this, 508 kg is associated with the cryogenics (Irace and Rosing, 1983).

The spacecraft would move an appropriate distance, perhaps a few kilometers, from Space Station, and the two light collectors would point at the source to be studied. Crude relative positioning of the major optical elements would be followed by fringe search and acquisition. This process would be done with the spacecraft at a small separation to assure high initial fringe contrast. Concern about moving large spacecraft in such close proximity to one another is legitimate; for the system to work at all, however, station-keeping must be maintained to within microns. Unless this requirement is met, the device is useless. With a properly designed experiment, one can insure that failure of one or all on-board systems will not lead to collision.

Either one or two dimensional measurements can now be made. For comparatively bright sources (mode 1), full image reconstruction can be achieved if the light collecting satellites are flown in a spiral of constantly increasing diameter so that measurements of fringe contrast and position as functions of color can be obtained over a grid of positions. The fringe contrast and position information are used to obtain image Fourier transform amplitudes and phases. The inverse transform yields an image of the source with a resolution, in radians, of order λ/D

where λ is the wavelength of the light and D is the maximum distance between light collecting spacecraft. λ/D is also the resolution of a single monolithic aperture of diameter equal to the maximum spacecraft separation.

We have calculated that a 0.5 newton thruster permits a pair of 1.0-meter optical collectors with individual masses of 1000 kg to completely fill the area of a 100-meter equivalent aperture in 9 hours. We note that so finely-sampled a grid of measurements will not, in general, be necessary. The observing strategy is subject to significant optimization as a function of source. The visible wavelength resolution associated with a 100-meter aperture is 1 milliarcsecond, approximately 40 times that of Space Telescope. Five hundred meter spirals are possible for the thruster size and fuel use we have specified.

Because the predominant thrust requirement is provision of a centripetal force for the light collectors circling the central station, the use of tethers is an obvious possibility. Due to problems of interference with light beams and transmission of vibrations we have not considered their use here but combining tethers with thrusters would yield a significant fuel use advantage.

An alternate mode of operation (mode 2) is more appropriate to the case of faint sources, for which poor signal-to-noise in the fringes dictates slower spacecraft motions and longer integration times. In the case of these objects, one-dimensional measurements with very slow spacecraft drift rates represent the most efficient use of observing time. Very long one-dimensional baselines are a possibility at any light level above $\sim m_V = 19$, and for faint sources the signal-to-noise requirements are greatly relaxed by concentrating only on accurate measurement of the separation corresponding to the first fringe null, all that is needed to perform a diameter determination. The observing strategy described in Stachnik *et al.* (1983) suggests that selection of the proper orbital configuration permits very long baseline measurements with extremely small expenditures of fuel.

IV. POSITION SENSING, THRUSTER REQUIREMENTS AND VIBRATION CONTROL

It is clear that the chief technical problem to be solved is that of assuring sub-micron pathlength equality at the fringe sensor surface as the major optical elements move in a complex pattern through a differential gravitational field. Very high level precision thruster control is required and on-board vibration must be minimized. Residual contributions to path-length inequality must be sensed and compensated.

The most direct method of sensing path error depends upon measurement of the fringes themselves. Introduction of a one-wave differential path error will result in displacement of the fringe pattern by a fringe width. Problems arise when noise masks the fringe modulation used to generate the error signal. In the ideal case, the noise is due purely to quantum fluctuations and becomes a serious problem when the source brightness is low, when the fringe amplitude to be measured is small or when uncompensated vibrations or accelerations necessitate extremely short "exposure times."

We shall see in Sections V and VI that for full reconstruction of complex image structure it is necessary to measure fringes of very low contrast; however, the spectral cross-dispersal technique assures that, at some wavelengths, relatively high contrast fringes will always be available for error signal generation. At our maximum Fourier plane sampling rate, set by the available thrust of 0.5 nt, we suggest in Section VI a sampling time at each spacecraft separation and position angle of 3 seconds, and indicate that this will result in a photon count adequate for phase recovery for 8th magnitude stars. This limit is chosen to insure 1%, or better, measurement of fringe position over the integration time, the accuracy we believe necessary for sources of interest.

Is it possible to insure a high degree of pathlength stability over the 3-second integration period? Several levels of sensing and correction are available to help satisfy this condition. The pathlength correction systems include the thrusters themselves, the optical delay line (which may incorporate both fine and coarse correction loops), active piezo vibration damping of key structures, and post-detection fringe drift compensation of the sort described at the end of Section II. Sources of error signals, other than the fringes themselves, include precision accelerometers, piezo structural vibration sensors, piezo thrust sensors and modeling of thruster effects and residual vibrations.

Thruster uniformity requirements vary with frequency range. For the case of rigid bodies at least, the large inertia and small thrust of the engines make the spacecraft surprisingly insensitive to large thrust fluctuations at high frequencies. Forces required to produce 0.02μ displacements (0.04 of a fringe at a wavelength of 0.5 μ) are given below as a function of frequency.

Thruster Force Error Required
to Produce a 0.02μ Displacement Error
(1000-kg Rigid Spacecraft)

Integration Time (sec)	Force Error (nt)
0.01	4×10^{-1}
0.1	4×10^{-3}
1.0	4×10^{-5}
10.0	4×10^{-7}

If correction updates are available every 3 seconds, we require 4μnt thrust uniformity of our 0.5-nt thruster. Thrusters in this range exist at present.

Typical bi-propellent thrusters have 2-5% thrust uniformity over a wide range of frequencies (Sutherland and Maes, 1966). An accepted technique for obtaining higher uniformity is to use a "layered" system consisting of a large thruster which produces the basic impulse and a smaller thruster which, when provided with the appropriate error signal, compensates, at the several percent level, for fluctuations in the larger device. Three to five layers would provide the uniformity required here. The lowest thrust "layer" could be provided by variable reflectivity micro-shutters changing both reflectivity and reflectivity angles of the skins of the different spacecraft (Labeyrie, *et al.* 1982, C.E.H., 1983).

Each thruster layer is mounted through a piezo strain gauge measuring the force provided by that particular motor. The resulting measurement force for each motor provides control signals for the next lower level of thruster. The entire propulsion package is mounted through a strain gauge monitoring overall force uniformity. At the lowest frequencies, the applied force measurements might be supplemented by signals from precision accelerometers of the sort used in the Discos (Johns Hopins, 1974), Cactus (Bernard *et al.*, 1982), and Super-Cactus (Bernard *et al.*, 1982) experiments. Super-Cactus is a particularly interesting device since it is capable of measuring accelerations as small as 10^{-11}m/sec. Super-Cactus is, however, non-linear in response, having its full sensitivity only at low accelerations. Devices having a similar sensitivity at accelerations as high as 10^{-5}m/sec^2 (Bernard *et al.*, 1982) are projected for the near future. This approaches typical SAMSI accelerations of 5×10^{-4}m/sec^2. Accelerometers measure only non-gravitational effects, however, and derivation of positions from accelerometer data also require modeled differential gravitational potential information derived from ultra-precise gravity gradiometer maps. In general, we believe that the best and most practical method of relative position determination will be fringe measurements.

Continuous operation of the thrusters even at a modest thrust level, suggests the use of a high specific impulse propulsion system. A liquid hydrogen-liquid oxygen (LH_2-LOX) combination has a specific impulse of 460 sec (Forward, 1983), and a 67 kg. propellant mass would assure continuous 0.5 nt operation for a week. Assuming that only a top-level thruster, having a ±3% thrust uniformity, uses LH_2-LOX, and that lower-level thrusters use much more controllable but less efficient cold gas technology, the maximum additional propellant would be 26 kg. per week.

Use of cryogenic propellants has the disadvantage of requiring large dewars. In the case of IRAS, 75 kg. of liquid helium required a 432-kg. dewar (Irace and Rosing, 1983). IRAS, however, had a hold-time of 12 months; we require a hold-time of a week. Furthermore, the more easily held liquid oxygen would presumably provide a jacket for the liquid hydrogen. The resulting dewar design could be considerably lighter and less sophisticated. Cryogenic material will be required, as well, for measurement of signals in the thermal infrared and the same cryogenic reservoir feeding the propulsion system can supply, as well, an LH_2-LOX fuel cell supplementing the estimated 500 watts available from solar cells covering the bodies of the light collectors. No additional power may be needed, since 500 watts is all the power required by IRAS.

The foregoing suggests that reasonable amounts of fuel can be carried by the SAMSI spacecraft for a week's observing. This time may be extended significantly if use of tethers, now under study, proves practical. When fuel levels become unacceptably low the spacecraft would return to Space Station for refueling.

Experiments reported by Forward (1980, 1981a, 1981b) describe considerable success in sensing extremely minute vibrations in structures by means of piezo strain gauges of the type used in gravity wave detectors. The appropriate signals are then sent to other piezo devices, used as drivers rather than sensors, in order to achieve active mechanical damping of the structure. The result has been damping of vibrations in optical systems of as much as three orders of magnitude over a range from ten to 5000 Hz. Forward (1980) states that measurements corresponding to differential displacements of 10^{-6} microns, one tenth the diameter of an atom, have been made and that in one experiment, active damping of a membrane mirror support was so good that, with the damping loop closed, reflections from the mirror were identical whether or not vibrations were being excited in the support. This promising technology can be extended to frequencies below 1 Hz (Forward, 1983).

V. PHASE MEASUREMENT AND IMAGE RECONSTRUCTION

The problem of full image recovery using Michelson interferometry has been less extensively studied than has the simpler case of determining source angular diameters. This is true because the latter problem requires only measurement of the light collector separation at which fringe contrast drops to zero (the contrast rises again for larger separations). Full image reconstruction requires both fringe contrast and phase measurements (to be described shortly) at many position angles and separations at far larger baselines, for which the contrast drops to perhaps a few tenths of a percent.

Ground-based measurements of such extremely low contrast features are complicated by the fact that the atmosphere imparts severe, and randomly changing, distortions to the wavefronts transmitted to the central station by the light collecting elements. An early approach to minimizing this problem was to pick off a small portion of wavefront of characteristic size, r_o, for which

$$1 \text{ cm} \lesssim r_o \lesssim 10 \text{ cm}.$$

Over r_o the distortion is small and the wavefront may be regarded as essentially plane. The rapid and random pathlength changes remain, however, and the same size of r_o means that few photons are available for interference. Ingenious alternative schemes have been devised permitting use of larger portions of the wavefront but they must still contend with unpredictable pathlength fluctuations and, in general, pay the price of measuring not the fringe contrast directly but, rather, the square of this quantity. This is not a serious shortcoming when one wishes only to locate a first null, but, when the measured modulation is very low, the signal-to-noise may be too poor for even extremely bright sources.

Comparison with the circumstances surrounding space-based Michelson is striking. The wavefronts are as plane as available optical technology can make them. Vibrations are readily modeled and can, in any case, be directly measured by highly sensitive piezo sensors. There is no atmospheric absorption of light outside the visible range and there is no need for amplitude-square measurement techniques.

Furthermore, in space, in the absence of random wavefront deformations, a technique proposed for use on the ground by Koechlin (1977), to use distortions in dispersed fringes in the measurement of Fourier transform phase, becomes far more powerful. The problem in measuring very small displacement of a fringe from the geometric equi-path position, corresponding to zero phase, is in determining the reference position. Koechlin pointed out that the technique of Labeyrie (1980) by which fringes are dispersed along their length to permit simultaneous measurement of contrast over a range of wavelengths contained a possible solution. Since resolution varies as λ/D, the resolution at a given light collector separation is a linear function of wavelength. It is, in fact, possible for an object to be unresolved at one wavelength and well resolved at another. Since a completely unresolved point has no structure contributing to fringe displacement, the zero phase reference provided by a star observed at one wavelength may be used to measure phase displacement at other wavelengths. "Wiggles" as a function of wavelength (shown in Figure 6) become markers of phase as a function of wavelength. This sort of differential procedure becomes still more powerful when a very large range of wavelengths can be simultaneously measured. Array detectors exist over a spectral range extending from 0.1 to 18 μ, and there is no reason, in principle, why this entire region cannot be observed. Furthermore, this implies a resolution ratio of 180:1 at a single baseline.

In fact, of course, complications exist. Detector sensitivity curves, source spectral distributions and changing source morphology as a function of wavelength make both measurement and interpretation of fringe wiggles difficult. Very high contrast fringes ($\gtrsim$ 15%) exist only for the case of an unresolved source. Thus, such very high contrast fringes can always be taken to mark a zero phase reference. Obviously, even if they occur in disadvantageous spectral emission or detector response regions, very high contrast fringes can be easier to measure than low contrast fringes.

If no high contrast fringes can be measured at adequate signal-to-noise anywhere in the spectral range, the problem becomes somewhat more difficult in that selection of the best approaches to phase recovery may depend upon having some knowledge of the object. In the very prelimianry experiments we have done, described in Section VI, model dependency seems very weak. For stellar-type sources, local maxima of the fringe amplitudes occur at locations where the phase takes on values near either 0 or $\pm \pi$. Information on detailed source structure, in the form of fringe "wiggles" occurs away from these maxima. It is possible, that reference phases may always be relatively easy to find, with zero displacement occuring at specifiable amplitude maxima.

We note that accurate recovery of the phases is far more important in successfully inverting the Fourier transform to obtain an image than is accurate measurement of the amplitudes (Andrews and Hunt 1977). We undertake discussion of the problems of measuring both in the next section.

VI. SIGNAL-TO-NOISE ESTIMATION FOR SAMPLE SOURCES

The "magnitude limit" of SAMSI will depend on details of the system technical characteristics, numerous specifics of the observing protocol (including spectral bandwidth and integration time) and nature of the source. Furthermore, as we have already indicated, full image recovery (mode 1) has far more stringent signal-to-noise requirements than does simple diameter determination. The limiting magnitude will therefore differ substantially. We have not yet attempted a full signal-to-noise analysis. What follows is an extremely simple examination of the general character of the fringe behavior combined with reasonable assumptions about system characteristics in an effort to arrive at preliminary estimates of visible wavelength magnitude limits for both observing modes.

Figure 7 shows several model stars for which we investigated the general behavior of the associated fringe patterns. All are characterized by limb darkening coefficients of 0.5 and between 15 and 20 circular surface features ranging in size between 6% and 35% of the stellar diameter. Feature contrasts vary in the range 10% to 40% One star, C, has a random, 10% modulation granulation pattern. The stars are 32 resolution elements in diameter.

Figures 8a, 9a, 10a, and 11a show the associated fringe (Fourier transform) amplitudes and 8b, 9b, 10b, and 11b show fringe phases along one dimensional cuts. Most ground-based long-baseline interferometry concerns itself with measurement of the location of the first null and the secondary maximum. Full image reconstruction at a resolution corresponding to 32 elements across the stellar disk requires measurement of the entire curve shown in these figures. The horizontal "spatial frequency" scale could equally well be labeled "light collector separation" or "baseline." For a circular source, the first null occurs at a baseline of 1.22 λ/α, where λ is the wavelength and α, the source angular diameter in radians. Thus, our four sample images depict the 5000Å wavelength resolution one might achieve with a 100-meter baseline for a 33-milliarcsecond diameter star.

In addition to amplitude cuts, we have also generated phase cuts. Each amplitude null is associated with a π phase change. For a completely centro-symmetric object, these changes are discontinuous. For more complex stellar surfaces, how-

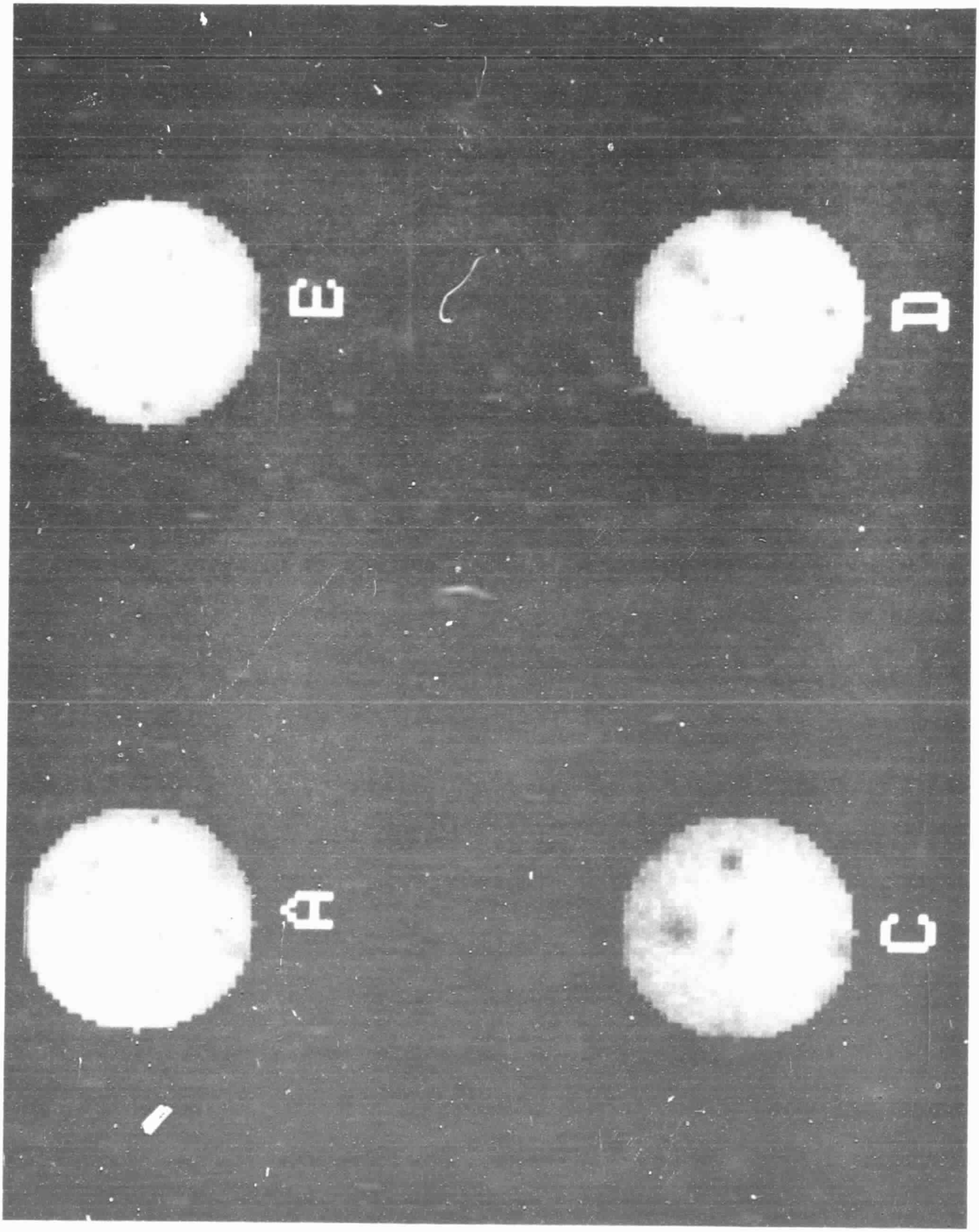

Fig. 7

ever, the phase assumes values near either zero or $\pm\pi$ only when the amplitude is at a maximum and otherwise takes on intermediate values. For the 16384 point two-dimensional Fourier transforms associated with the four images in Figure 7, histograms of the phase show that over half are within $\pm$ 0.03 radian of zero and 10% are within $\pm$ 0.03 Radian of $\pm\pi$. For a fringe phase resolution of $\pm$ 0.10 radian, 25% of the measured phases are seen to have values different from zero or $\pm\pi$. It is these values that carry information on the non-centro-symmetric image structure. As we have already pointed out, accurate phase recovery appears (Andrews and Hunt, 1977) to be of greater importance than accurate determination of the amplitudes. Clearly, the foregoing does no more than to suggest the level to which measurements must be made for reconstruction of surface features to be possible. It is of interest to estimate the magnitude of a star for which phases can be determined to within $\pm$ 0.10 radian.

After Hardy and Wallner (1979) for the case of direct-not quadratic-fringe contrast measurement, and with contrast reduction due to photon statistics alone, the RMS fringe amplitude and phase measurement errors, σ_{γ_A} and σ_ϕ are given by

$$\sigma_{\gamma_A} = \frac{\sqrt{3}}{\sqrt{N}}$$

$$\sigma_\phi = \frac{\sqrt{3}}{\sqrt{N\gamma_A}}$$

where N is the number of detected photons in a measurements interval and γ_A is the image Fourier transform amplitude. σ_{γ_A} measures the fringe contrast error relative to the contrast at $\gamma_A = 1$ and σ_ϕ measures the phase error at a given fringe contrast, γ_A, in radians.

Inspection of the Fourier transform amplitude curves suggests that fringe contrasts in the range 0.005 to 0.001 must be measured in order to obtain useful information. At a fringe contrast of 0.003, 10^5 photons are required for $\pm$ 0.1 radian

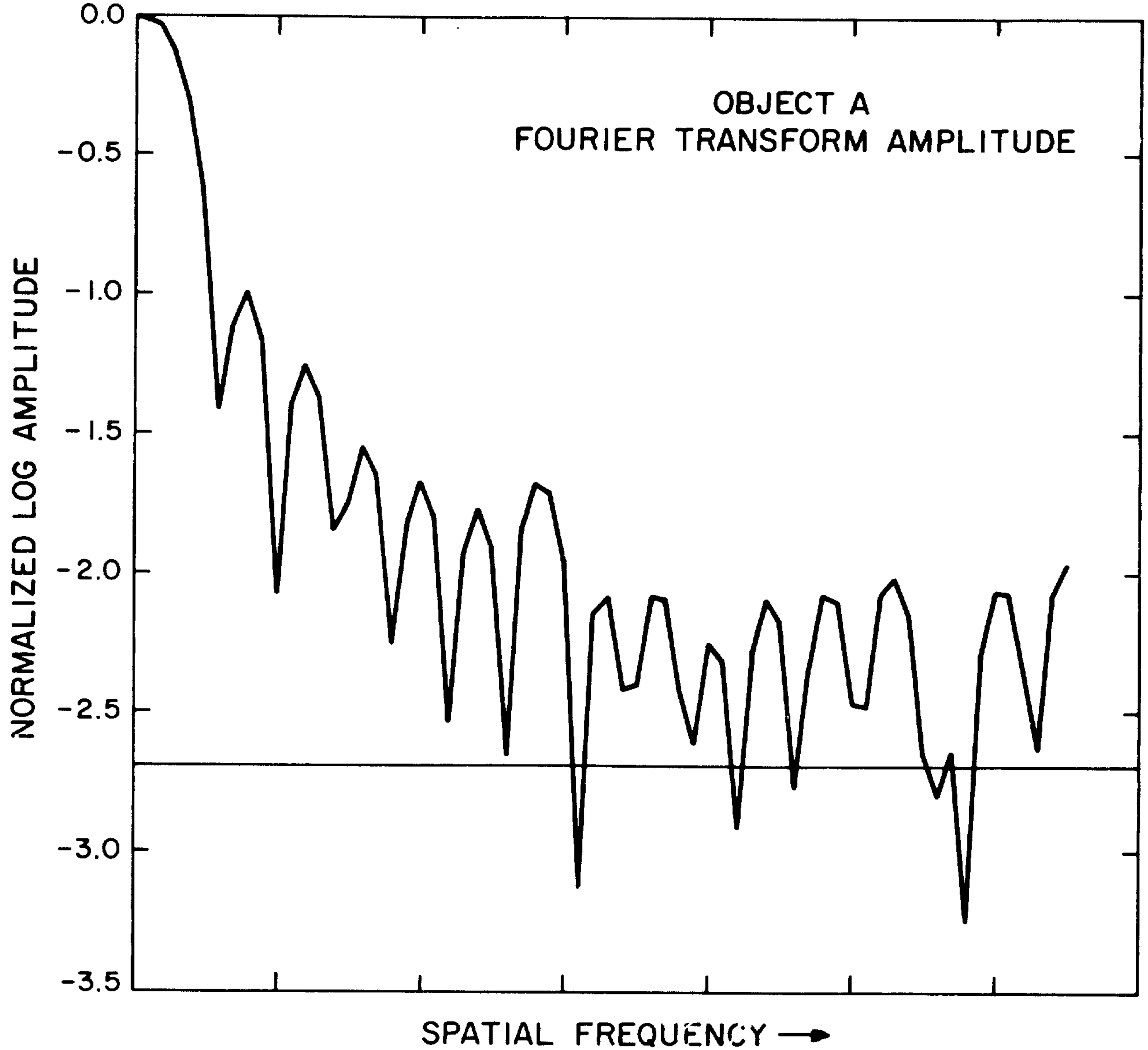
OBJECT A
FOURIER TRANSFORM AMPLITUDE
0.0
-0.5
-1.0
-1.5
-2.0
-2.5
-3.0
-3.5
NORMALIZED LOG AMPLITUDE
SPATIAL FREQUENCY

Fig. 8a

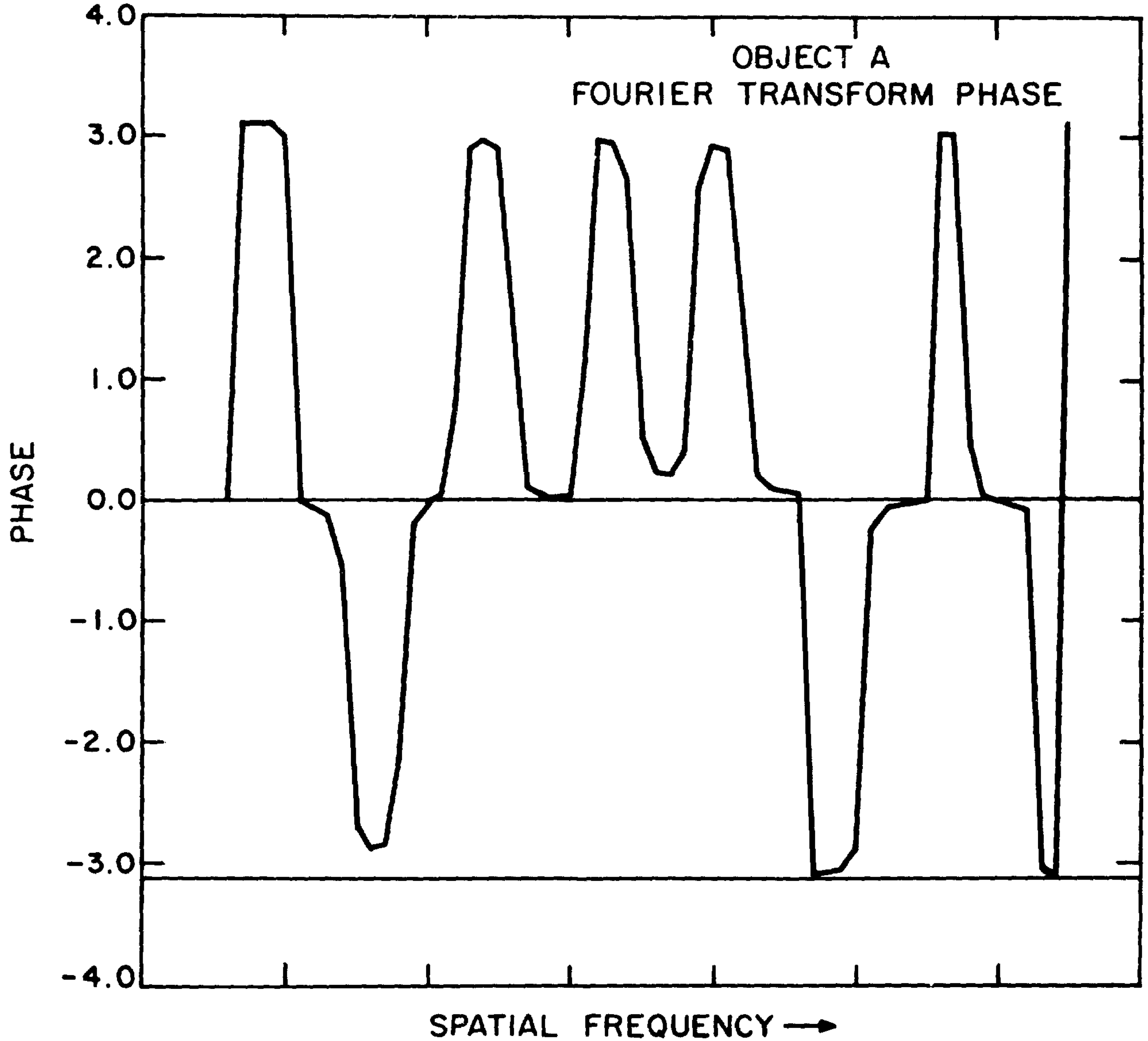

ORIGINAL PAGE IS
OF POOR QUALITY

Fig. 8b

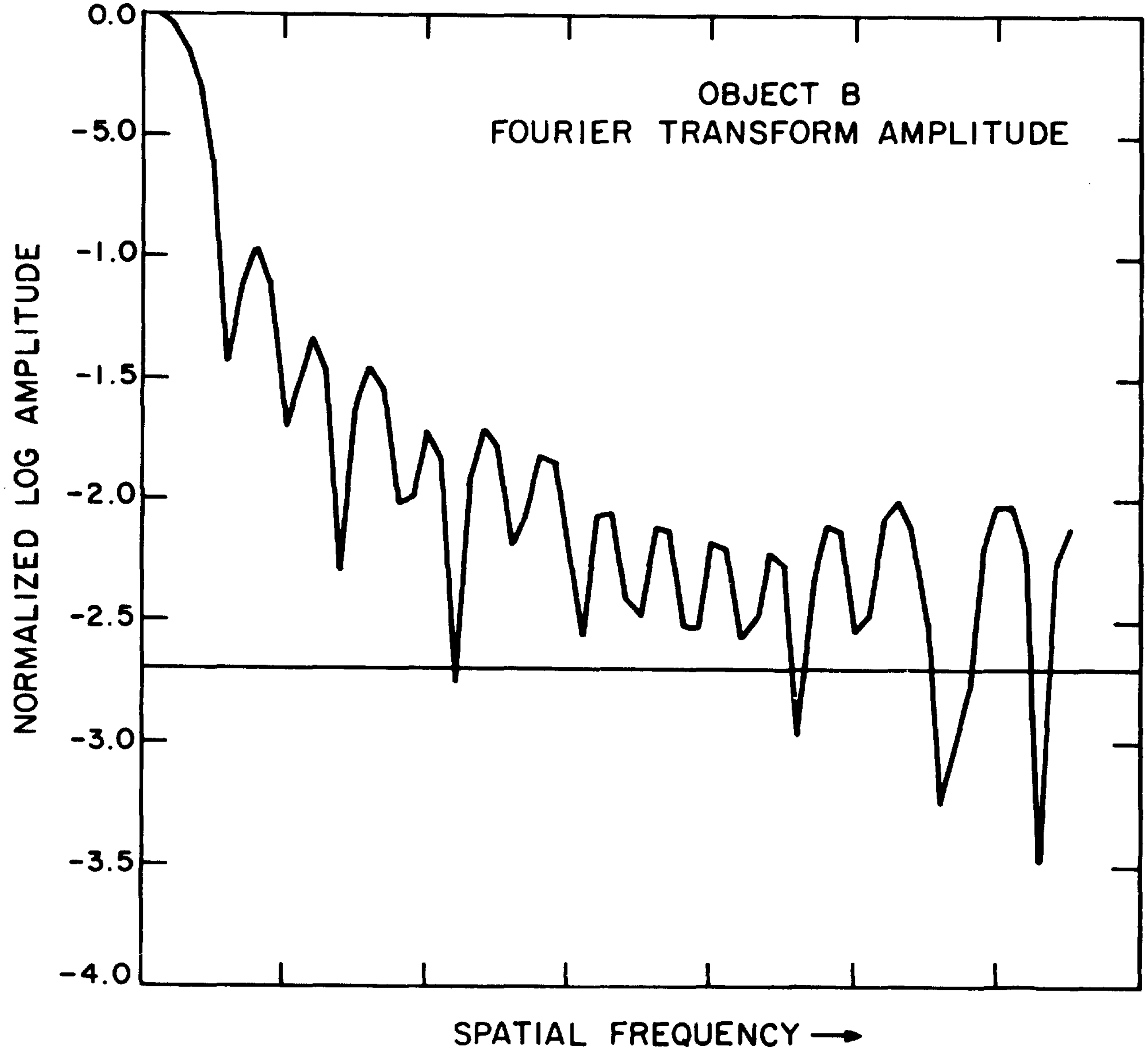
OBJECT B
FOURIER TRANSFORM AMPLITUDE
0.0
-5.0
-1.0
-1.5
-2.0
-2.5
-3.0
-3.5
-4.0
NORMALIZED LOG AMPLITUDE
SPATIAL FREQUENCY

Fig. 9a

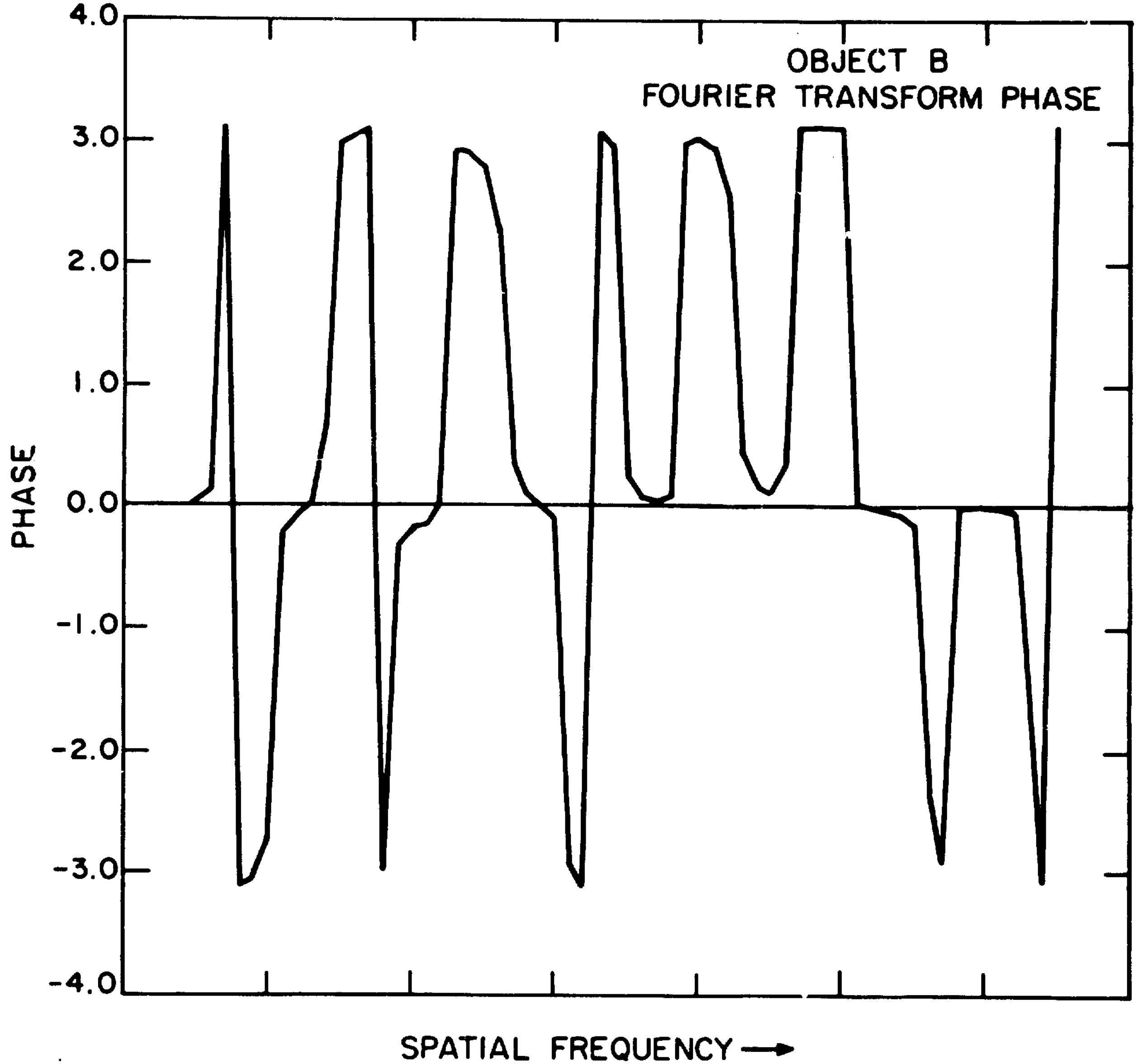
4.0
3.0
2.0
1.0
0.0
-1.0
-2.0
-3.0
-4.0
PHASE
OBJECT B
FOURIER TRANSFORM PHASE
SPATIAL FREQUENCY

Fig. 9b

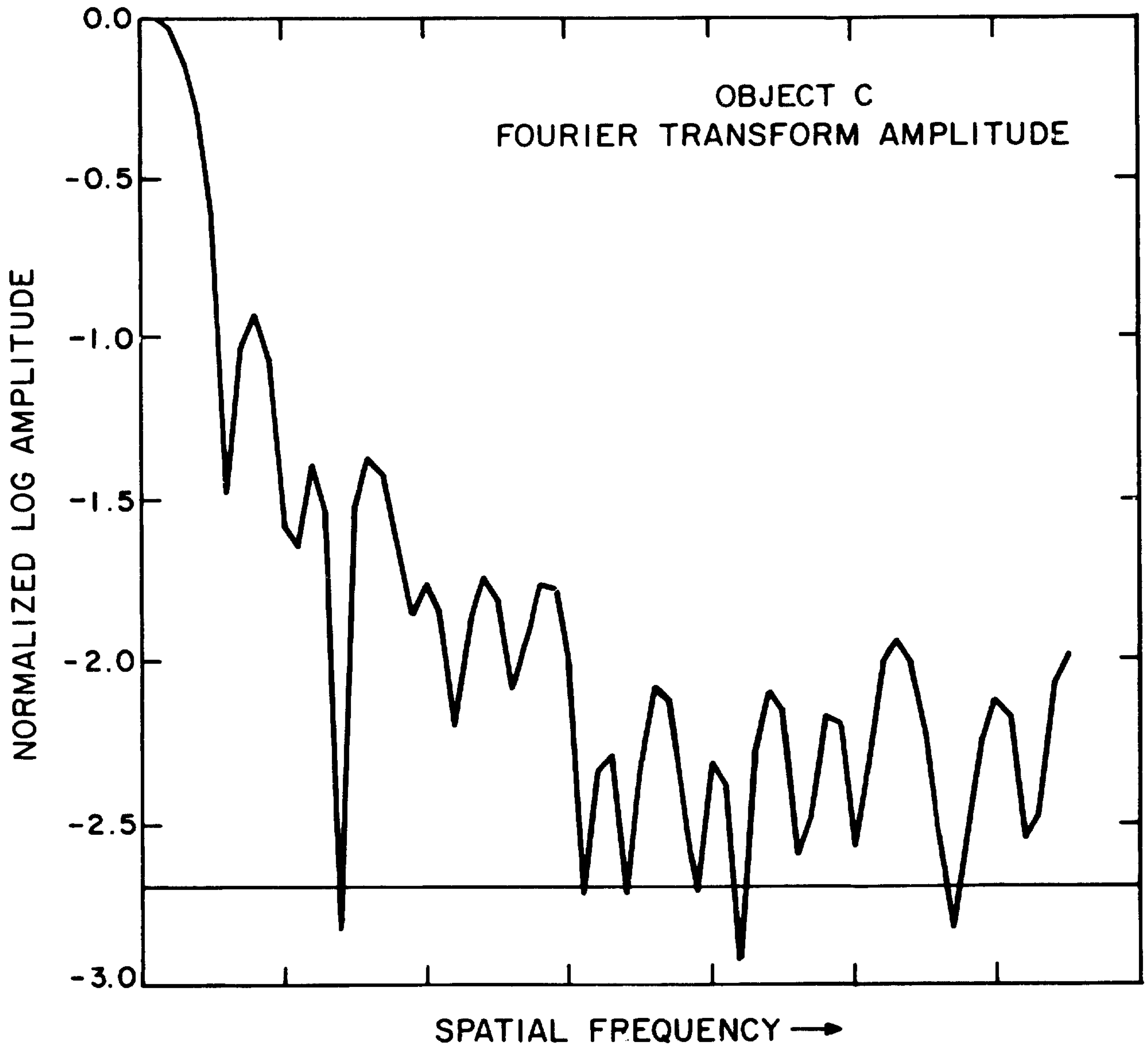

OBJECT C
FOURIER TRANSFORM AMPLITUDE
0.0
-0.5
-1.0
-1.5
-2.0
-2.5
-3.0
NORMALIZED LOG AMPLITUDE
SPATIAL FREQUENCY

Fig. 10a

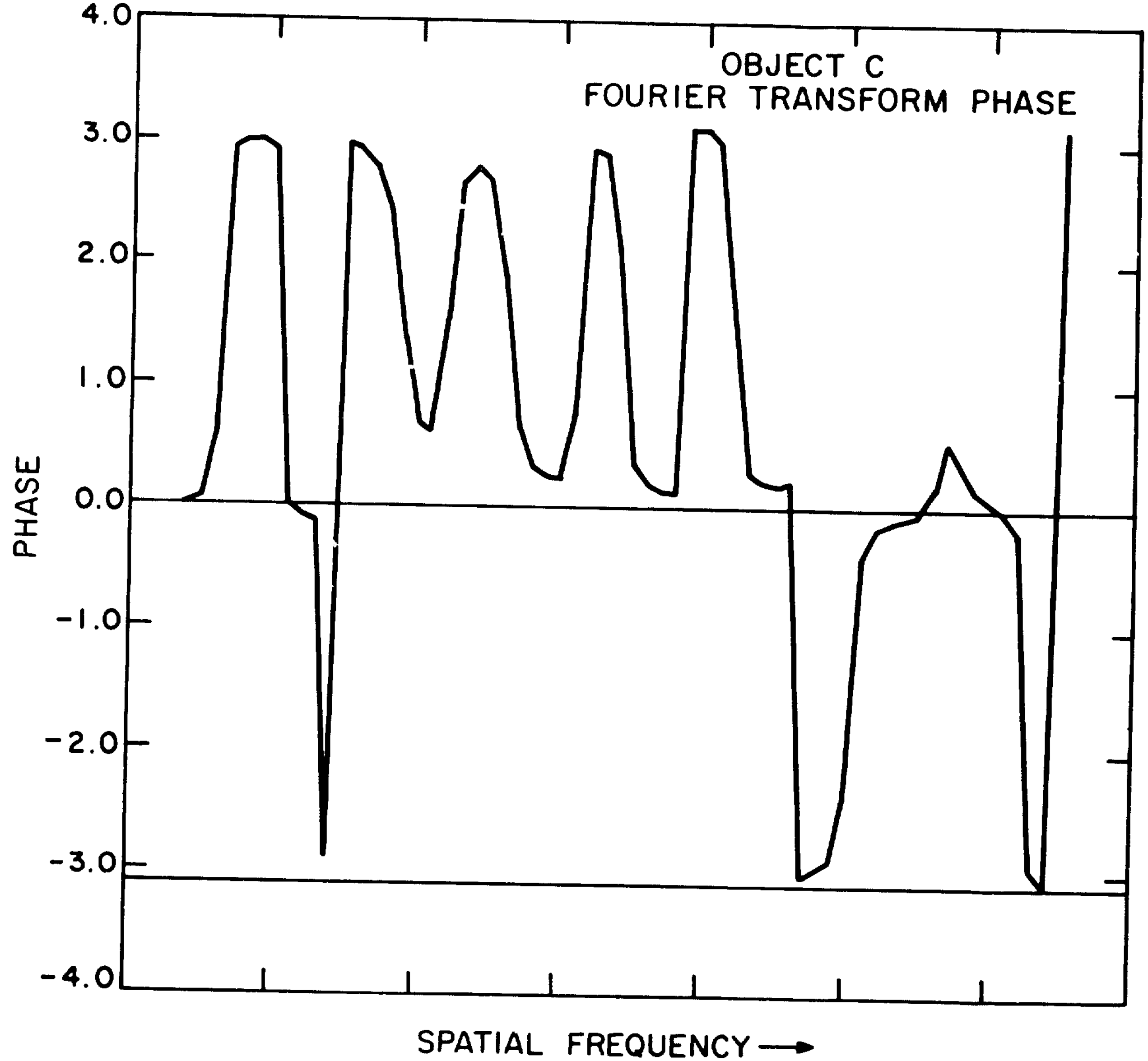
OBJECT C
FOURIER TRANSFORM PHASE
4.0
3.0
2.0
1.0
0.0
-1.0
-2.0
-3.0
-4.0
PHASE
SPATIAL FREQUENCY

Fig. 10b

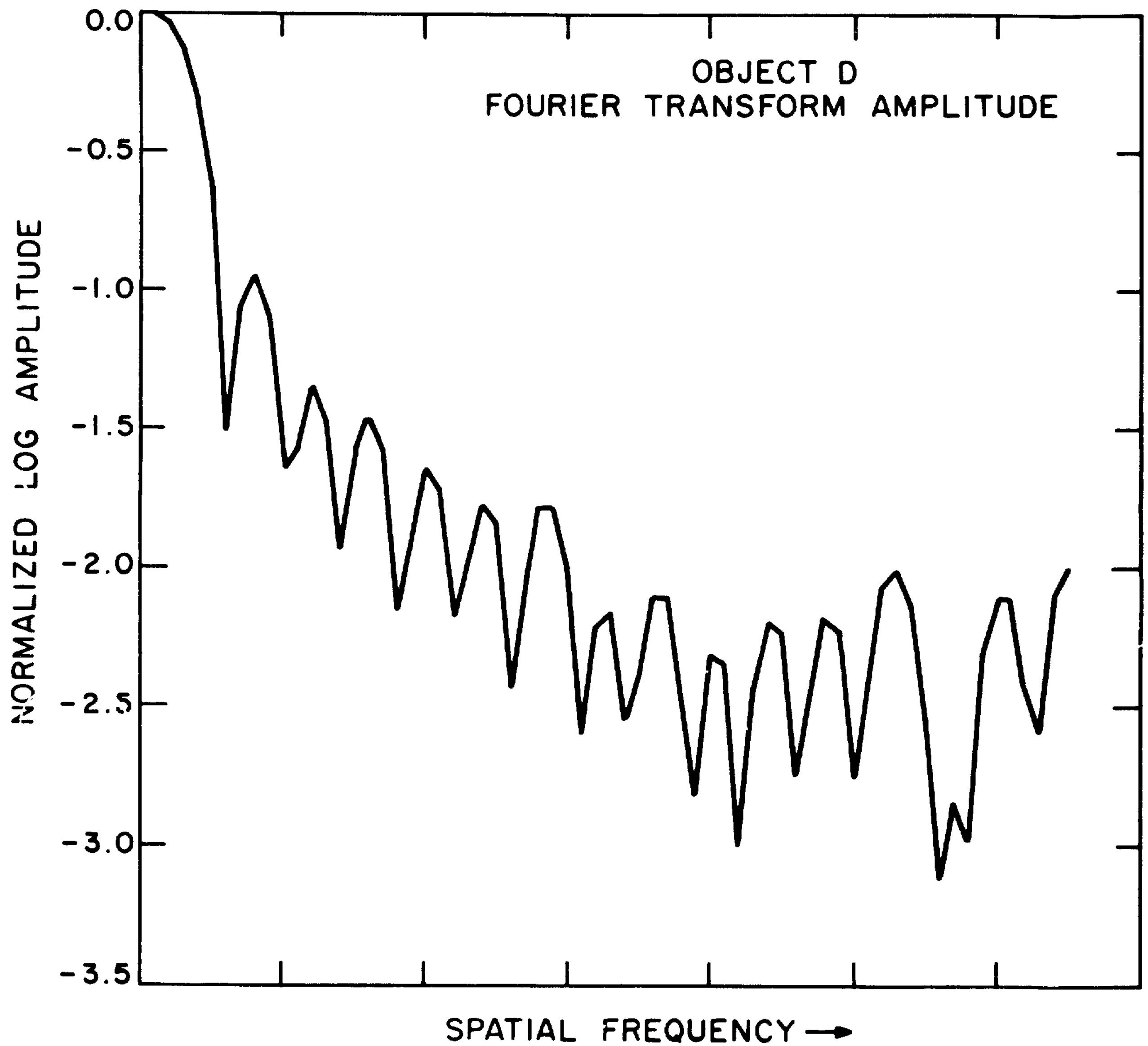
OBJECT D
FOURIER TRANSFORM AMPLITUDE
0.0
-0.5
-1.0
-1.5
-2.0
-2.5
-3.0
-3.5
NORMALIZED LOG AMPLITUDE
SPATIAL FREQUENCY →

Fig. 11a

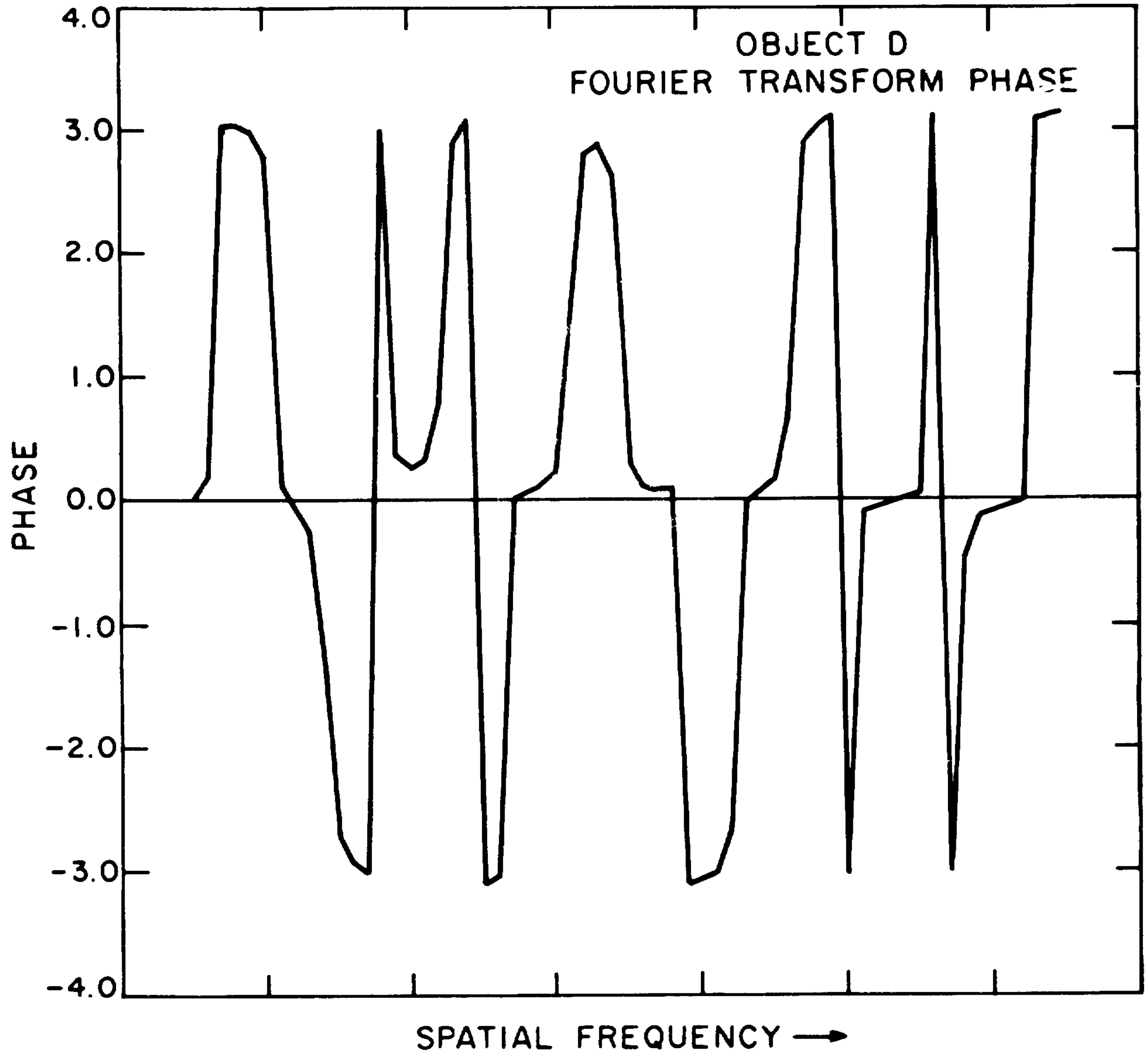

OBJECT D
FOURIER TRANSFORM PHASE
4.0
3.0
2.0
1.0
0.0
-1.0
-2.0
-3.0
-4.0
PHASE
SPATIAL FREQUENCY

Fig. 11b

phase measurement.

Figure 12 shows number of detected photons per 100Å spectral band for stars belonging to eight spectral types. The assumed spectral response is that of an S-20 photocathode. The eight stars have the same V-magnitude (note that the curves cross at $\lambda = 0.54\mu$). Other assumptions include:

- 2 one-meter telescopes
- $m_V = 5$
- Integration time = 3.0 sec.
- Optical efficiency = 0.2

The 3-sec integration interval allows time for 11000 samples in Fourier space during a 9-hour observing period. For the case of the 100-meter spiral, typical light collector velocities are 0.15 m/sec, implying spacecraft motion in a 3-second interval of approximately half an aperture width. The restriction of a 3-sec maximum integration time is set by the 0.4μ-nt/integration time thrust uniformity-controllability requirement already discussed.

It is clear that, for all spectral types, many more than 10^6 photons are present in each 100Å spectral band for the specifications used in Figure 12. At this same 100Å bandpass, stars 3 magnitudes fainter could be measured over a spectral range of at least several thousand angstroms. This implies imaging in tens of spectral bands simultaneously. A magnitude limit of 8 includes all stars resolvable at baselines of several hundreds of meters. For sufficiently bright stars, it is possible to narrow the bandpass to permit acquisition of, in effect, "spectroastrograms"–single spectral line stellar images.

For the case of simple angular diameter determination (observing mode 2), we need only measure fringe contrast to within 10% in order to insure detection of the secondary maximum. Thus, since,

$$\sqrt{N} = \frac{\sqrt{3}}{\sigma_{\gamma_A}} = \frac{\sqrt{3}}{0.1} = \sqrt{300}$$

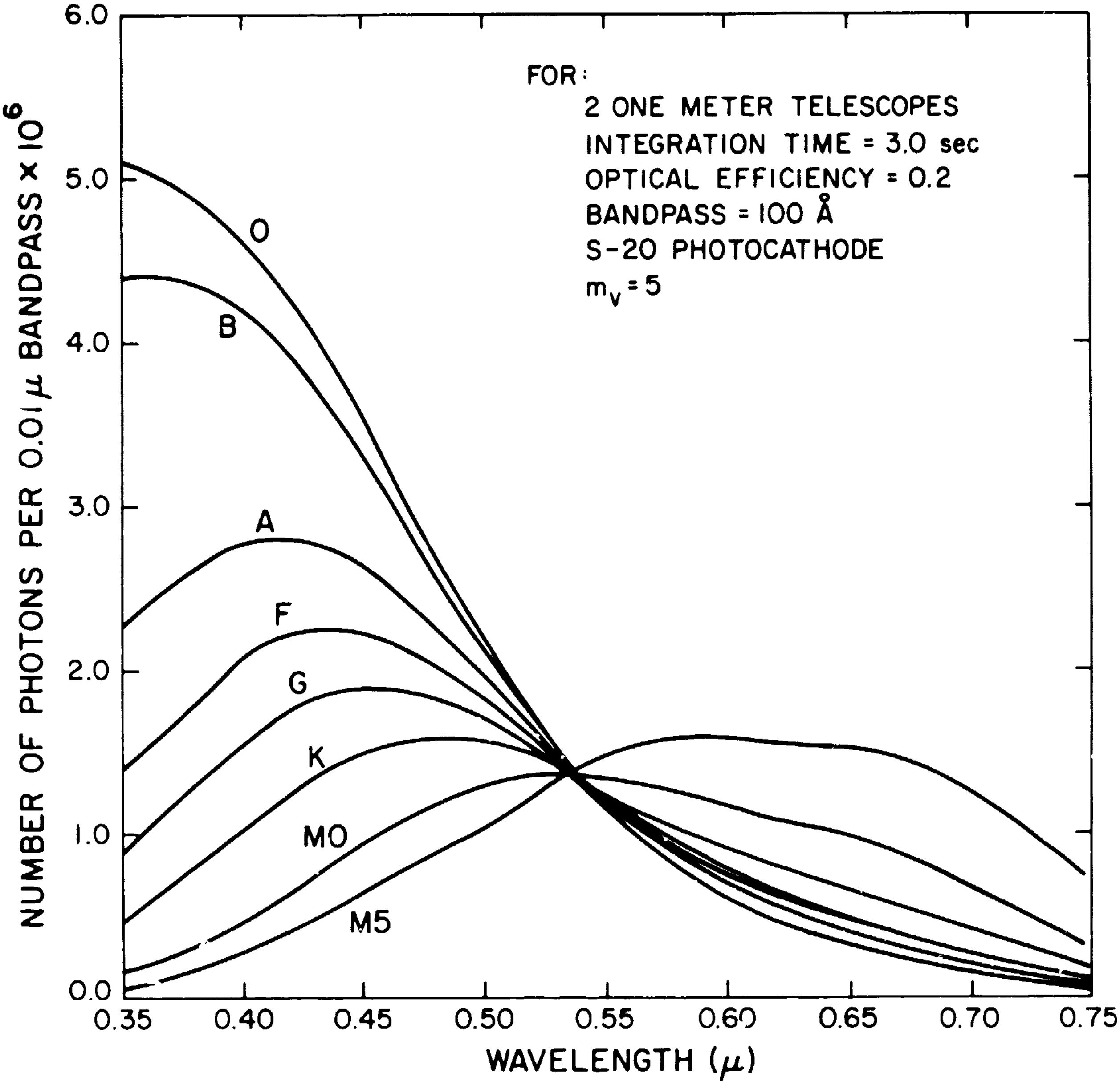

FOR:
2 ONE METER TELESCOPES
INTEGRATION TIME = 3.0 sec
OPTICAL EFFICIENCY = 0.2
BANDPASS = 100 Å
S-20 PHOTOCATHODE
$m_V = 5$
O
B
A
F
G
K
MO
M5
NUMBER OF PHOTONS PER 0.01μ BANDPASS × 10^6
WAVELENGTH (μ)
6.0
5.0
4.0
3.0
2.0
1.0
0.0
0.35
0.40
0.45
0.50
0.55
0.60
0.65
0.70
0.75

Fig. 12

300 photons per measurement are required.

Figure 12 shows that at least 1.5 x 10^6 photons are available from a 5th magnitude source under the specified observing conditions. Increasing both the bandpass and integration time by an order of magnitude is permissible (for one dimensional measurements, the propulsion system, the principal source of unmodeled fringe wander, can largely be shut down in favor of using differential orbital effects to move the spacecraft), bringing the photon flux to 1.5 x 10^8, 14 magnitudes brighter than is needed for diameter determination only. Given the stated conditions, then, we have a magnitude limit of 19.

Diameter determination alone, for very large baselines (> 10 km), has already been explored by us with the aid of NASA "Center of Excellence" and "Innovative Research Program" funding (Stachnik *et al.* 1983). All of the findings of that earlier study apply to the system described here. The key result of that work was that, for one-dimensional spatial measurements, extremely favorable orbital configurations exist, for which "automatic" baseline scanning is obtained with only very limited expenditure of fuel. Even for the full 10 km baseline, a new object can be studied every 90 minutes. All of the functions of the original design, with the addition of full imaging, can be fulfilled with the present system.

Compared to full image reconstruction with its more limited baseline and less favorable magnitude limit, this second observing mode has at least as great, or greater, a scientific importance.

VII. ASTROPHYSICAL APPLICATIONS

The astrophysical applications of SAMSI differ considerably depending on which of the two observing modes--full image reconstruction or one-dimensional power spectrum measurements--is being discussed. The high information density and ease of interpretation characterizing the former is offset by its less favorable magnitude limit, longer data collection time and more limited resolution.

In the full imaging mode, expected resolutions are as follows:

Resolution in Microarcseconds

Baseline (m)	Wavelength (m)			
	0.1	0.5	5.0	20.0
100	0.2	1.0	10.0	40.0
500	0.04	0.2	2.0	0.6

† The magnitude limit is at least 8.

Perhaps a half-dozen supergiants have angular diameters sufficiently large to permit visible wavelength resolution of 30 elements with a baseline of 100 meters. Surface structure on several hundred stars could, however, be monitored at 32-element resolution, at a baseline of 500 meters. This need require only a slightly longer observing time and a modest increase in full usage. Such imaging, especially in narrow spectral bands and with time-sequences, could contribute significantly to our appreciation of the solar-stellar connection. At a 500 meter baseline, betelgeuse would be resolved at over 150 resolution elements.

In general, angularly large stars are cool and above the main sequence. With the 500-meter baseline, we estimate that 30-element resolution is possible for main sequence stars as early as late-F. Lesser resolution is, of course, possible for still earlier stars. Resolution is, in principle, possible for later-type stars but problems could arise because the (approximately) 10-hour measurement time becomes a significant fraction of the stellar rotation period.

Comparatively detailed studies of additional astrophysical applications of very high angular resolution measurements appear in a doctoral thesis (Vatoux 1979) and, in English translation, in a manuscript by Praderie (1979), in Davis (1979), and in Field *et al.* (1981).

Full image reconstruction will be possible for stellar surfaces, close, and perhaps interacting, binary stars and circumstellar gas and dust emission features. In general, this observing mode will be most appropriate to problems of stellar physics and dynamics, for which light levels are high. A more complete evaluation of the scientific implications of full imaging at these resolutions over a very wide range of wavelengths will be carried out in a future study.

The second observing mode, for which very high resolution, one-dimensional measurements, are posible, has been studied in more detail.

The resolution achievable with an (expandable) 10-km one-dimensional baseline is at least 10^{-5} arcsecond. This is five orders of magnitude greater than is typical of routine earth-based measurements and several orders greater than may be expected from other near-term space or ground-based imaging techniques. Meaningful extrapolations regarding the likely significance of such ultra high-resolution observations have dubious value but it is possible to make some useful statements.

10^{-5} arcsecond resolution is adequate to resolve an earth-sized object at 10 pc, a white dwarf at 40 pc, and the Sun at 1000 pc. Supergiants could be resolved in nearby galaxies. With good signal-to-noise ratio, stellar limb darkening can be measured and some inferences drawn about the presence of surface structure for stars far smaller than those which can be imaged. It would be possible to measure directly angular diameters for stars of <u>all</u> spectral and luminosity classes. Simultaneous multi-color observations are a a natural consequence of our interferometer design. Where direct distance measurements are available, reliable linear diameters can be obtained, and one is left with the prospect of a powerful geometric distance indicator calibrated in a very straightforward manner against nearby stars. The number of specific astrophysical problems for which such information would be useful is very large.

Within the galaxy, interesting measurements would result from studies of such prosaic sources as rotationally-flattened stars and contact binaries and such exotic objects as SS 433, (perhaps at a larger baseline) the Crab optical pulsar, and expanding nova shells at a very early stage in the explosion. In all cases, simultaneous collection of infrared and ultraviolet data would permit a far deeper understanding of the underlying physical processes in these systems.

A list of extragalactic objects for investigation would certainly include quasars and galactic nuclei as well as, at somewhat larger baselines, individual sources within nearby galaxies. The expanding shell due to a supernova explosion in a nearby galaxy would be observable within hours of the beginning of an outburst. Extending the galactic measurements, there is the prospect of developing geometric distance indicators to tie intragalactic distances to local group extragalactic distance (using stars) and using geometric measures of quasars or galactic nuclei to check or buttress conjectures about the large scale structure of the universe.

VIII. MICRO-SAMSI

Studies have now been undertaken for two versions of SAMSI. The original large-scale design had as its goal acquisition of large numbers of one dimensional spatial power spectrum measurements for different objects, at very high (10^{-5} arcsec) resolution, with a high observing efficiency (16 objects/day). The current Space-Station associated version, known internally, for a time, as "mini-SAMSI", would fulfill all of the functions of the original SAMSI but would also make use of the resupply capability of Space Station to replenish micro-rocket propellants needed to move the SAMSI spacecraft through the more complex maneuvers required for full image reconstruction.

In order both to assess the technology requirements of the larger systems and to undertake some extremely interesting scientific experiments in the relatively near term, it would be useful to consider a still smaller device, micro-SAMSI. Micro-SAMSI would be a Shuttle-deployed package incorporating as many design simplifications as possible while still retaining the essential feature of SAMSI -- a multiple spacecraft approach with potential for very high angular resolution measurements.

The design simplifications would include elimination of the following capabilities of the version of SAMSI described in this report: observation over a wide wavelength range, measurement of extremely low contrast fringes, Fourier transform phase recovery, in-space refuelling and high-speed, high-efficiency two-dimensional image Fourier transform sampling. Micro-SAMSI might rely heavily on tethers or booms for spacecraft motion, have a simpler fine pointing system and be designed primarily for measurement of high contrast fringe amplitudes at a small number of position angles on bright sources. This would still permit simple angular diameter measurements, including limb darkening, for hundreds, possibly thousands, of stars.

We hope to pursue a study of micro-SAMSI as part of a phased program leading to eventual development of a full scale imaging device.

IX. FUTURE STUDIES AND LABORATORY EXPERIMENTS

Studies of SAMSI so far have concentrated on determining that plausible solutions exist for problems arising in all relevant technical sub-areas. Future investigations should concentrate on detailed analysis in a more limited number of key technology areas. Four such areas stand out:

- Study of the image reconstruction problem with signal-to-noise analysis and computer simulation.
- A laboratory study of the fringe measurement and active path length compensation problems.
- Detailed orbital analysis for the required complex spacecraft mo-

tion in a differential gravitational field with special attention given to use of tethers.

- Scientific assessment of experiments possible in the full imaging mode of operation.

To date, extremely valuable technical contacts have been developed with European scientists in France, Germany and the United Kingdom working on a parallel project under ESA auspices. We would like to explore future involvement with a NASA Center and, perhaps, with industry technical representatives.

ACKNOWLEDGEMENTS

This work was done with the assistance of Keith Ashelin, of M.I.T., soon to be with the Los Angeles Air Force Station. Sharron Hamilton, of Wellesley College, also participated. Beryl Langer was the artist for the color illustration.

REFERENCES

Andrews, H.C., Hunt, B.R. 1972, *Digital Image Restoration.*

Bernard, A., Gay, M., and Quillerat, R. 1982, *The Cactus Accelerometer*, AGARD Do-graph No. 254, 5-1.

Bien, F., Comac, M., Caulfield, H.J., and Ezekiel, S. 1980, *Ap. Opt.*, **20**, 400.

Bourdet, G.L., and Orszog, A.G. 1979, *Ap. Opt.*, **18**, 225.

Colombo, G., Arnold, D.A., Binsack, J.H. (MIT-CSR), Gay, R.H., Grossi, M.D., Lautman, D.A., and Orringer, O. (MIT-CSR) 1976, *SAO Report in Geoastronomy No. 2.*

Davis, J. 1979, *The Application of High Angular Resolution Interferometry to the Study of Single Objects,* Proceedings of IAU Colloquium No. 50, ed. J. Davis and W.J. Tango, Chatterton Astronomy Dept., Univ. of Sydney, NSW, Australia.

Dunn, R.B. 1980, *Proceedings: Optical and Infrared Telescopes for the 1990's,* Adelaide Hewitt, Kitt Peak National Observatory, Tucson, AZ, 156.

Elson, B.M. 1973, *Av. NK. and Sp. Tech.*, **98**, 53.

Field, G., Katz, J., Muller, R.A., Press, W., Shapiro, I. 1981, *Working Paper of the Astrophysics Working Group*, Nat. Acad. Sci. study.

Forward, R.L. 1979, *Ap. Phys.*, **51**, 5601.

Forward, R.L., and Swigert, C.J. 1981, *J. Spacecraft*, **18**, No. 1, 5.

Forward, R.L. 1981, *J. Spacecraft*, **18**, No. 1, 11.

Forward, R.L. 1983, personal communication.

Hardy, J.W., and Wallner, E.P. 1979, *Active Controlfor Michelson-Stellar Interferometers,* Proceedings of IAU Colloquium No. 50, ed. J. Davis and W.J. Tango, Chatterton Astronomy Dept., Univ. of Sydney, NSW, Australia, 10-1.

Hill, P.G., and Peterson, C.R. 1965, *Mechanics and Thermodynamics of Propulsion*, 371.

Irace, W. and Rosing, D. 1983, *J. British Interplanetary Soc.*, **36**, 27-33.

John Hopkins University Ap. Phys. Lab. Staff, Space Dept., and Stanford University

Staff, Guidance and Control Lab., *J. Spacecraft*, **11**, No. 9, 637.

Jones, C.O. 1979, *Opt. Eng.*, **18**, 273.

Kibblewhite, E.J. 1979, report submitted to ESA.

Koechlin, L. 1977, *Optical Telescopes of the Future*, , ESO Conference, Geneva, Switzerland, 475.

Labeyrie, A. 1980, *Proceedings: Optical and Infrared Telescopes for the 1990's*, ed. Adelaide Hewitt, Kitt Peak National Observatory, Tucson, AZ, 786.

Labeyrie, A., Savaria, E., and Schumacher, G. 1982, *Flute or Trio: Different Approaches to Optical Arrays in Space*, IAU Symposium on VLBI, Toulouse, France.

Papaliolios, C., Mertz, L. 1982, *Instrumentation in Astronomy IV, SPIE Vo. 331*, 360.

Praderie, F. 1979, *Angular Interferometry from Space*, unpublished report of meetings and experiments of French astronomers at Meudon and CERGA.

Querzola, B. 1979, *Ap. Opt.*, **18**, 3035.

Stachnik, R.V., Melroy, P., McCormack, E.F., Arnold, D., and Gezari, D.Y. 1982, *Instrumentation in Astronomy 5*, SPIE Proceedings, 445-52.

Stachnik, R.V., and Labeyrie, A. 1984, Optical Astronomy from Clusters of Satellites, *Sky and Telescope*, scheduled for publication February.

Sutherland, G.S., and Maes, M.E. 1966, *J. Spacecraft and Roc.*, **3**, No. 8, 1153.

Tango, W.J., Twiss, R.Q. 1983, *Progress in Optics*, **17**, 241.

Vatoux, S.A. 1979, *Etude Theoretique et Experimentale d'un Interferometre Stellaire Optique, a Usage Spatial*, Doctoral Thesis, submitted to Universite de Paris-Sud, Centre d'Orsay.

FIGURE CAPTIONS

Figure 1. Schematic diagram of a Michelson stellar interferometer. Light from widely-separated locations on the wavefront of a star are combined at the surface of a detector. If the pathlengths are equal to within a few microns, fringes, whose contrast are determined by the baseline and by the angular diameter of the source, are observed. Spectral dispersion out of the plane of the page permits simultaneous fringe measurements over a wide spectral range.

Figure 2. Illustration of the spiral pattern flown by SAMSI during image reconstruction, following deployment from Space Station, described in the text.

Figure 3. Central station functional schematic diagram, showing a pair of back-to-back telescopes which track the two light-collector satellites. Light transmitted to the central station interferes and fringe contrast is measured as a function of separation of the light collectors. Figure is from an earlier study in which ion, rather than chemical, thrusters were the primary propulsion devices.

Figure 4. Schematic diagram of one of the light-collector satellites, showing how a converged and collimated beam from the source is transmitted to the central station. The electric propulsion system, shown here, would be replaced by LH_2/LOX thrusters.

Figure 5. Central station optical schematic diagram.

Figure 6. Dispersed fringes falling on area detector arrays spanning a spectral range from 0.1 to 18.0 microns.

Figure 7. 4 stellar images for which Fourier transform phase and amplitude characteristics were studied. All stars have 32-element resolution, a 0.5-limb-darkening coefficient and between 15 and 20 surface

spots having a range of sizes and contrasts.

Figures 8, 9, 10 and 11, A and B. Fourier transform amplitude and phase cuts, respectively, for the stellar images in Figure 7.

Figure 12. Numbers of photons per 100Å passband in the spectral interval 0.35 to 0.75 microns for stars of 8 spectral types. Other parameters are specified on the figure.